Loss-of-expression FLC alleles derived from weedy radish facilitate the development of highly florigenic rootstocks for graft-mediated floral induction

Ko Motoki

ko.motoki.3f@okayama-u.ac.jp

Okayama University: Okayama Daigaku https://orcid.org/0000-0001-7740-3949

Saki Kobayashi

Okayama University: Okayama Daigaku

Kazusa Nishimura

Okayama University: Okayama Daigaku

Yu Kinoshita

Kyoto University: Kyoto Daigaku

Makoto Kashima

Toho University: Toho Daigaku

Koichiro Ushijima

Okayama University: Okayama Daigaku

Tanjuro Goto

Okayama University: Okayama Daigaku

Ken-ichiro Yasuba

Okayama University: Okayama Daigaku

Munetaka Hosokawa

Kindai University: Kinki Daigaku

Research Article

Keywords: Graft-mediated floral induction, FLOWERING LOCUS C (FLC), FLOWERING LOCUS T (FT), vernalization, weedy 53 radish (Raphanus raphanistrum), Brassica oleracea

Posted Date: October 27th, 2025

DOI: https://doi.org/10.21203/rs.3.rs-7792339/v1

Title

Loss-of-expression *FLC* alleles derived from weedy radish facilitate the development of highly florigenic rootstocks for graft-mediated floral induction.

Author information

Ko Motoki[1*], Saki Kobayashi[1], Kazusa Nishimura[1], Yu Kinoshita[2], Makoto Kashima[3], Koichiro Ushijima[1], Tanjuro Goto[1], Ken-ichiro Yasuba[1], Munetaka Hosokawa[4,5]

[1]Graduate School of Environmental, Life and Natural Science and Technology, Okayama University, 1-1-1 Tsushima-naka, Kita-ku, Okayama City, Okayama 700-8530, Japan

[2]Graduate School of Agriculture, Kyoto University, 4-2-1, Shiroyamadai, Kizugawa City, Kyoto, 619-0218, Japan

[3]Faculty of Science Department of Biomolecular Science, Toho University

[4]Faculty of Agriculture, Kindai University, Nara, 631-8505, Japan

[5]Agricultural Technology and Innovation Research Institute Kindai University (ATIRI), Nara, 631-8505, Japan

Corresponding Author

Ko Motoki

E-mail: ko.motoki.3f@okayama-u.ac.jp

ORCID: https://orcid.org/0000-0001-7740-3949

Author Contributions

Conceptualization: KM, YK, MH; Data curation: KM, SK, KN, MK, KU; Formal analysis: KM, KN, YK, MK, KU; Funding acquisition: KM; Investigation: KM, SK, KN, MK, KU; Methodology: KM, KN, YK, MK, KU; Project administration: KM; Resources: KM, KN, MK, KU, TG, KY, MH; Software: KN, MK; Supervision: KM, YK, TG, KY, MH; Validation: KM, SK, YK; Visualization: KM, SK, KN, YK, KU; Writing – original draft: KM, SK, YK, – review & editing: KN, MK, KU, TG, KY, MH.

Acknowledgements

Radish seeds were kindly provided by the Genebank Project, NARO, Japan, and Tohoku University *Brassica* Seed Bank (listed in Table S1). We thank Dr. Tetsuya Nakazaki and Dr. Ryohei Nakano at Kyoto University for his valuable comments, and Dr. Hidetaka Nishida at Okayama University for supporting the RT-qPCR analysis.

Abstract

Graft-mediated floral induction is a classical yet promising breeding technique that accelerates seed production and shortens generation time in crops with long life cycles. However, its application is still limited to a few species due to the instability or failure of floral induction. Although genetic variation in floral induction ability of rootstocks has been reported, the underlying natural genetic factors remain unclear. Here, using a Brassicaceae grafting model, we investigated two early-bolting radish (*Raphanus sativus*) accessions differing in their ability to induce flowering. We focused on a significant difference in *FLOWERING LOCUS T* (*FT*) expression between these accessions, leading to the identification of two quantitative trait loci (QTLs) associated with *FT* levels. Transcriptomic and genomic analyses revealed that both QTLs harbored previously unreported loss-of-expression alleles of *FLOWERING LOCUS C* (*FLC*) homologs, key floral repressors involved in vernalization. Grafting experiments with F_2 populations demonstrated that these *FLC* loss-of-expression alleles enhanced floral induction additively, with *RsFLC1* having a stronger effect. Our results confirmed that successful graft-mediated floral induction requires *FT* expression exceeding the threshold for rootstock flowering itself. This elevated *FT* expression level can be accomplished by the substantially reduced repressive activity of *FLC* homologs. Further analysis revealed that these alleles originated from weedy radish (*Raphanus raphanistrum*), likely contributing to early flowering of these weeds in disturbed environments. This study demonstrates that identifying natural genetic variants that markedly enhance *FT* expression is an effective strategy to develop highly florigenic rootstocks, thereby broadening the application of graft-mediated floral induction in crop breeding.

Keywords

Graft-mediated floral induction, *FLOWERING LOCUS C* (*FLC*), *FLOWERING LOCUS T* (*FT*), vernalization, weedy radish (*Raphanus raphanistrum*), *Brassica oleracea*

Key message

Loss-of-expression *FLC* alleles from weedy radish act as expression QTLs for *RsFTa*, enabling florigenic rootstocks with strong graft-mediated floral induction for Brassicaceae crop breeding.

Introduction

Graft-mediated floral induction is a phenomenon in which flowering is induced in recipient plants under non-inductive conditions, by grafting them onto florally induced donor plants. This phenomenon was first described by Chailakhyan (1936) during his studies on the transmissive floral signal produced in the leaves, following the discovery of photoperiodism by Garner and Allard (1920). Since then, graft-mediated floral induction has been extensively studied as a model for understanding the transmission of systemic floral signals in plants (Lang 1952; Zeevaart 1976). It is now well established that this phenomenon is caused by the movement of florigen, specifically the FLOWERING LOCUS T (FT) protein and its homologs synthesized in the leaves of plants under inductive conditions. FT protein travels through the graft junction from the donor plant to the shoot apex of the recipient plant, where it induces flowering by activating downstream floral meristem identity genes (Corbesier et al. 2007; Lifschitz et al. 2006; Lin et al. 2007; Notaguchi et al. 2008).

Graft-mediated floral induction has long been considered as a potential technique for breeding and seed production, enabling forced flowering under non-inductive conditions. For example, in sweet potato (*Ipomoea batatas*), which rarely flowers in temperate regions, grafting onto related species such as moonflower (*Ipomoea alba*) or morning glory (*Ipomoea nil*) has been developed and is still used for hybrid breeding today (Kobayashi and Nakanishi 1982; Lam and Cordner 1955). In the 1960s, grafting onto related wild species was reported to induce flowering in late-bolting cultivars of sugar beet (*Beta vulgaris*) (Curtis and Hornesey 1964; Curtis 1964). Since the discovery of FT, grafting approaches using FT-overexpressing transgenic plants as rootstocks have also been explored, including successful examples in orange (*Citrus sinensis*) (Soares et al. 2020) and *Jatropha curcas* (Tang et al. 2022; Ye et al. 2014).

Although graft-mediated floral induction has long been recognized, its practical application in breeding remains limited to a few plant species. In some species, flowering is not induced even when scions are grafted onto florally induced rootstocks (van de Pol 1972). Similar failures have also been reported when transgenic plants overexpressing FT are used as rootstocks, with reports in trifoliate orange (*Citrus trifoliata*) (Wu et al. 2022), cassava (*Manihot esculenta* Crantz) (Bull et al. 2017; Odipio et al. 2020), poplar (*Populus* spp.) (Zhang et al. 2010), and apple (*Malus* × *domestica* Borkh.) (Tränkner et al. 2010; Wenzel et al. 2013). In these cases, the FT-overexpressing rootstocks themselves exhibited early flowering, suggesting that the lack of induction in grafted plants may result from insufficient FT movement from rootstock to scion (Putterill and Varkonyi-Gasic 2016), although the precise cause remains unclear. Together, these findings underscore the practical challenges of graft-mediated floral induction in breeding programs.

We developed a grafting technique that enables stable and early flowering of cabbage (*Brassica oleracea* L.), which normally requires a long period for floral induction due to its juvenility and strong vernalization requirement (Motoki et al. 2019, 2024). We found that certain early-bolting radish (*Raphanus sativus* L.) accessions can induce flowering in cabbage more effectively, which correlated with their higher FT protein supply compared with other radish or *B. oleracea* rootstocks (Motoki et al. 2022). It was shown that differences in FT protein supply capacity were associated with variation in *FT* gene expression levels and size of leaves, which is the organ responsible for FT protein production. We proposed this technique as the "GRAFT" method (Grafting onto Relatives capable of Abundant Florigen Transmission), emphasizing

the importance of selecting plants with high florigen supply capacity as rootstocks (Motoki et al. 2024). This technique has recently been adopted by several seed companies to accelerate the breeding of Brassicaceae crops.

The genetic basis underlying high *FT* expression level in radish accessions with strong floral induction ability remains unclear. Clarifying this mechanism is essential for developing rootstocks that enable faster and more reliable graft-mediated flowering. In the model plant *Arabidopsis thaliana*, *FT* expression is regulated by a range of environmental and endogenous cues, including photoperiod, vernalization, ambient temperature, plant age, and phytohormones (Kinoshita and Richter 2020). These signals are transduced through complex transcriptional networks involving multiple upstream regulators. Natural genetic variations affecting *FT* expression level have been reported across diverse plant species. These include mutations in the *cis*-regulatory regions of the *FT* locus itself (*A. thaliana*, Liu et al. 2014; *B. rapa*, Nishikawa et al. 2023; *C. sativus*, Wang et al. 2020; *G. max*, Zhao et al. 2016; *O. sativa*, Ogiso-Tanaka et al. 2013), as well as in *trans*-acting upstream regulators (*B. rapa*, Nishikawa et al. 2023; *G. max*, Xia et al. 2012; *O. sativa*, Takahashi et al. 2009; *Z. mays*, Huang et al. 2018).

Recently, a pan-genome of the genus *Raphanus* was released, revealing the genomic characteristics of its constituent species (Zhang et al. 2021). This pan-genome includes six varieties of the cultivated species *R. sativus*, two subspecies of the wild species *R. raphanistrum*, and interspecific hybrids between *R. raphanistrum* and *R. sativus*. All accessions possess nine chromosomes, and while the overall chromosomal arrangement is largely conserved across genomes, both inter-chromosomal and intra-chromosomal rearrangements were observed in some cases (Zhang et al. 2021). The use of a pan-genome facilitates the functional genomics, by enabling efficient detection of larger structural variants, such as presence/absence variants, copy number variants, inversions and translocations, which are often difficult to identify using traditional single-reference genomes (Shi et al. 2023).

In this study, we explored the genetic factors responsible for the high *FT* gene expression level in radish to elucidate the mechanisms underlying the natural variation in the graft-mediated floral induction ability. Quantitative trait loci (QTL) analysis on *FT* expression levels, combined with pan-genome-base comparison, identified two genomic regions, both harboring naturally occurring loss-of-expression alleles of *FLC* homologs. Grafting experiments demonstrated that these loss-of-expression alleles of *FLC* contributed to the variation in floral induction ability of the radish rootstocks by enabling early onset and constitutively high expression of *FT*, with differing magnitudes of effect. Further analysis revealed that these alleles originated from weedy radish (*R. raphanistrum*), likely contributing to their early flowering trait in disturbed environments. This study demonstrates that identifying natural genetic variants that enhance *FT* expression is an effective strategy to develop highly florigenic rootstocks, thereby providing a framework to broaden the application of graft-mediated floral induction in crop breeding.

Methods

Plant materials and population construction

R. sativus G2-IL1 (an inbred line of seedpod-harvesting type radish isolated from accession no. 76703, Genebank Project, NARO, Japan) and CH-IL1 (an inbred line of the seedpod-harvesting type radish isolated from cultivar

'Rat-tailed', Chiltern Seeds, United Kingdom) were used for the generation of segregating population. The G2-IL1 × CH-IL1 F_1 was obtained by crossing of the two accessions, and F_2 seeds were produced by self-pollinating a single F_1 individual. Self-pollination was performed using CO_2 treatment to overcome self-incompatibility, following the methods of previous studies (Nakanishi and Hinata 1975). Several radish accessions from Genebank Project and Tohoku University *Brassica* Seed Bank (https://www.agri.tohoku.ac.jp/pbreed/Seed_Stock_DB/SeedStock-top.html) were used for genotyping the *RsFLC1* and *RsFLC3* loci (Table S1).

Growth conditions for flowering time evaluation

For flowering time evaluation of the F_2 population in controlled conditions, plants were grown in a growth room maintained at 22 ± 2°C in long-day (LD) conditions (16 h light / 8 h dark). Light was provided using fluorescent lamps (PPFD 120 μmol m^{-2} s^{-1}; NEC Lighting, Ltd., Japan). Seeds were sown on moist filter paper and germinated in the dark at 22°C for 1 day. The germinated seeds were then transplanted into 7.5 cm diameter plastic pots filled with granular rockwool (Nippon Rockwool Corp., Tokyo, Japan) and cultivated further in the growth room. All plants were irrigated and fertilized from below using a half-strength nutrient solution (Enshi-shoho, formulated by the National Horticultural Research Station, Japan). Flowering time was recorded as the number of days from transplantation to bolting, with a plant defined as bolted when the flowering stem reached 3 cm in height above the top of the hypocotyl. A total of 189 individuals were cultivated under identical conditions in four independent survey rounds (23, 47, 47, and 72 plants, respectively).

For flowering time evaluation of the F_3 population, plants were grown in an unheated greenhouse at Kizu Farm, Kyoto University. Seeds were sown on moist filter paper and germinated in the dark at 22°C for 1 day. On June 23, 2022, the germinated seeds were transplanted into 7.5 cm diameter plastic pots filled with nursery soil (Ikubyo-baido, Takii Seed Co., Kyoto, Japan) supplemented with 3 g/L of slow-release fertilizer (Long-total kaki No.1, ZEN-NOH, Japan). The pots were placed on benches in the greenhouse and watered regularly. Flowering time was recorded as the number of days from transplantation to bolting, with a plant defined as bolted when the flowering stem reached 5 cm in height above the top of the hypocotyl.

Gene expression analysis in the F_2 population

Leaf disks were collected from the tip of the largest leaf of each individual in the G2-IL1 × CH-IL1 F_2 population grown in the growth conditions described above, at 14 days after sowing, between Zeitgeber time (ZT) 15.5 and 16.0. Total RNA was extracted from the leaf samples using Sepasol RNA I Super G (Nacalai Tesque, Inc., Kyoto, Japan), purified with Econospin™ for RNA (Epoch Life Science, Missouri City, TX, USA), and reverse-transcribed using ReverTra Ace® qPCR RT Master Mix with gDNA Remover (Toyobo Co., Ltd., Osaka, Japan), in accordance with the manufacturer's instructions. Gene expression analysis was performed on 115 individuals from survey rounds 1, 2 and 3, after excluding two individuals from which RNA extraction failed.

One microliter of 20-fold diluted cDNA was then used as the template for quantitative reverse transcription-PCR (RT-qPCR). RT-qPCR was conducted using the THUNDERBIRD® SYBR® qPCR Mix kit (Toyobo Co., Ltd.) in

accordance with the manufacturer's instructions, with amplification performed on a LightCycler® 480 system (Roche Diagnostics K.K., Tokyo, Japan). The thermal cycling conditions were as follows: initial denaturation at 95°C for 5 minutes, followed by 40 cycles of 95°C for 10 seconds, 60°C for 30 seconds, and 72°C for 30 seconds. Amplification specificity was confirmed using melting curve analysis. All RT-qPCR primers used in this study are listed in Table S2.

Library preparation and sequencing for genomic analysis

For whole-genome sequencing of G2-IL1 and CH-IL1, genomic DNA was extracted from leaf tissue using the DNeasy Plant Mini Kit (Qiagen, Valencia, CA, USA). Library preparation was performed using the TruSeq DNA PCR-Free Sample Preparation Kit (Illumina, San Diego, CA, USA), and the libraries were sequenced on an Illumina platform using 151 bp paired-end reads, yielding an average sequencing depth of approximately 25× for G2-IL1 and 40× for CH-IL1.

For the long-read sequencing of CH-IL1, DNA was extracted from leaf tissue using the NucleoBond® HMW DNA (MACHEREY-NAGEL GmbH & Co. KG, Düren, Germany). Size selection was conducted using BluePippin high-pass size selection (Sage Science, Inc., Beverly, MA, USA). Library preparation was performed using Ligation Sequencing Kit V14 (Oxford Nanopore Technologies plc, Oxford, UK). Sequencing was performed on a PromethION 2 Solo (Oxford Nanopore Technologies plc), generating an average sequencing depth of approximately 100×.

For dpMIG-seq library construction of the F_2 population, genomic DNA was extracted from leaf tissue using the method described by Mizuno et al. (2020). The dpMIG-seq library was constructed following the protocol described by Nishimura et al. (2024), using the primer set PS1_4–5. The constructed libraries were sequenced on an Illumina platform, generating 151 bp paired-end reads for subsequent genotyping analysis.

Reference-based variant calling

For whole-genome sequencing of the parental accessions, raw FASTQ files were filtered and trimmed using Trimmomatic (Bolger et al. 2014) to retain reads with a minimum quality score of 20. The resulting 150 bp paired-end reads were aligned to one of the reference genomes from the radish pan-genome (Zhang et al. 2021) using the Burrows–Wheeler Aligner maximal exact match with default parameters (Li and Durbin 2009). The resulting SAM files were converted to BAM format and sorted using SAMtools (Li et al. 2009). Reads with four or more mismatches were removed, and only properly paired reads were retained using SAMtools. The filtered reads were used as input for elPrep (Herzeel et al. 2021) to mark and remove duplicates, perform base quality score recalibration (BQSR), and execute variant calling via its HaplotypeCaller module. Per-chromosome GVCF files were generated and subsequently combined using the GenomicsDBImport and GenotypeGVCFs functions of GATK v4 (Van der Auwera and O'Connor 2020). SNPs and indels were filtered based on standard hard-filtering parameters, and only high-confidence homozygous variants passing all filters were retained. Finally, variants were annotated for predicted functional effects using SnpEff (Cingolani et al., 2012).

For the dpMIG-seq analysis of the F_2 population, the first 17 bases at the 5′ end of each raw read—derived from the primer used in the first PCR of dpMIG-seq—were removed using fastp (Chen 2023) with parameters -f 17 -F 17,

along with quality trimming (-q 20) and filtering of low-quality reads (-n 10). Paired-end reads were also processed to remove polyG tails and adapters using the default settings of fastp. Processed reads were mapped to the RS00 reference genome using SNAP-aligner with default parameters for paired-end mode. The resulting BAM files were sorted and indexed using SAMtools. Variants were called using samtools mpileup with the -d 0 option, and passed to BCFtools (Danecek et al. 2021) for SNP/INDEL calling. The resulting VCF files were filtered using VCFtools to retain high-confidence biallelic variants with a minimum depth of 5, minor allele frequency of 0.1, and missing data threshold of 20%.

Linkage map construction and QTL analysis of the F_2 population

A linkage map of the F_2 population was constructed using Lep-MAP3 (Rastas 2017). Filtered VCF files were separated by chromosome, and polymorphisms within each chromosome-specific file were grouped using the SeparateChromosomes2 module of Lep-MAP3. For downstream analysis, the linkage group containing the highest number of markers per chromosome was selected as the representative linkage group. QTL analysis was performed using R/qtl (Broman et al., 2003). Composite interval mapping was applied to identify QTLs associated with days to bolting and the relative expression level of *RsFTa* normalized to *RsActin*. The significance threshold for the LOD score was determined using 1,000 permutation tests.

Genomic sequence analysis of *RsFLC1* and *RsFLC3* loci

To characterize the genomic sequences of *RsFLC1* and *RsFLC3* in G2-IL1 and CH-IL1, short-read resequencing data were mapped to 11 reference genomes from the radish pangenome (Zhang et al. 2021) using BWA-MEM with default parameters. Variants, including SNPs and indels, were called using the mpileup function in SAMtools, followed by variant calling with BCFtools. Homozygous polymorphisms within ORFs of *RsFLC1* and *RsFLC3* were counted to identify the most similar reference genome for each accession. Based on this analysis, RS00 and RS08 were selected for *RsFLC1*, and RS03 and RS09 for *RsFLC3* for further analysis. Genomic regions containing *RsFLC1* or *RsFLC3* along with their flanking sequences were retrieved and aligned using the nucmer tool from MUMmer4 to detect potential structural variants (Marçais et al. 2018).

For CH-IL1, long-read genomic data generated using Oxford Nanopore sequencing were aligned to the RS08 reference genome using minimap2 (Li 2018). Structural variations around *RsFLC1* were manually inspected using Integrative Genomics Viewer (Helga et al. 2013). Allele-specific genomic PCR primers targeting variants in *RsFLC1* and *RsFLC3* were designed based on the detected structural polymorphisms between G2-IL1 and CH-IL1 (Fig. S1, Table S2). PCR was performed using KOD One® PCR Master Mix (Toyobo Co. Ltd.) using the following conditions: 35 cycles at 98°C for 10 sec, 60°C for 5 sec, and 68°C for 7 sec. Allele-specific primers were mixed at equal concentrations in a single reaction to perform multiplex PCR for each gene.

RNA-seq library preparation and sequencing

RNA-seq analysis was performed using G2-IL1 and CH-IL1 plants grown under LD conditions in a growth room, as described above. Leaf disks were collected from the tip of the largest leaf of each plant at 14 days after sowing, between ZT 15.5 and 16.0 (n = 4 per accession). Total RNA was extracted from the sampled leaves using a modified version of the Direct-TRI method described by Ujibe et al. (2021), in which powdered frozen leaf tissue was homogenized in Sepasol RNA I Super G (Nacalai Tesque, Inc.), and RNA was subsequently purified using Econospin™ for RNA (Epoch Life Science). Non-targeted RNA-seq libraries were prepared using the Lasy-Seq ver. 1.1 protocol (https://sites.google.com/view/lasy-seq/) (Kamitani et al. 2019; Kashima et al. 2021). Sequencing was performed on an Illumina platform, generating 150 bp paired-end reads for downstream transcriptome analysis.

Mapping and gene quantification

Processing of the RNA-seq data was conducted following the method described by Kashima et al. (2021). Read 1 sequences were trimmed using fastp with the following parameters: --trim_poly_x -w 20 --adapter_sequence=AGATCGGAAGAGCACACGTCTGAACTCCAGTCA --adapter_sequence_r2=AGATCGGAAGAGCGTCGTGTAGGGAAAGAGTGT -l 31. The trimmed read 1 sequences were then aligned to the radish reference RNA sequence of RS00 (GWHANWD00000000.RNA.fasta) using BWA-MEM with default settings. Gene-level quantification was performed using Salmon (Patro et al. 2017) with the -l IU option to specify the library type. The resulting read counts per gene were summarized using R (version 4.3.2; R Core Team 2023). Differential expression analysis was carried out using the edgeR package (Robinson et al. 2010), applying the glmQLFTest function to identify DEGs. Genes with $|\log_2 FC| > 1$ (FDR = 0.05) were considered as differentially expressed. Homologs of 317 flowering time-related genes, compiled from Arabidopsis thaliana gene lists in the Flowering Interactive Database (FLOR-ID; Bouché et al. 2016) and the George Coupland group (https://www.mpipz.mpg.de/14637/Arabidopsis_flowering_genes), were identified in the RS00 reference genome through mutual BLAST searches.

Effect of *RsFLC1* and *RsFLC3* genotype on the floral induction ability of radish rootstocks

Grafting experiments were conducted in a growth room maintained at 22 ± 2°C under LD conditions (16 h light / 8 h dark). Light was supplied using daylight-color LED lamps at a PPFD of 120 μmol m^{-2} s^{-1}. Seven to ten individuals homozygous for specific *RsFLC1*/*RsFLC3* genotypes—$RsFLC1^{Lpt1}/RsFLC3^{Ngr1}$, $RsFLC1^{Lpt1}/rsflc3^{Rpn1}$, $rsflc1^{Ldr1}/RsFLC3^{Ngr1}$, and $rsflc1^{Ldr1}/rsflc3^{Rpn1}$—were selected from the F_2 population of G2-IL1 × CH-IL1 by genotyping with allele-specific primers, as described above. The selected plants were transplanted into 7.5 cm diameter plastic pots filled with granular rockwool (Nippon Rockwool Corp) and used as rootstocks. The grafting experiment was conducted in two replicates, with three to five individuals per genotype used in each replicate. Cabbage 'Matsunami' (Ishii Seed Growers Co., Ltd., Shizuoka, Japan) seedlings, 3 to 4 weeks after sowing, were used as scions. Split grafting was performed following the method of Motoki et al. (2022), when the radish seedlings had bolted to a height of 7 cm above the hypocotyl. Grafted plants were cultivated for 65 days after grafting.

To evaluate the floral induction ability of each rootstock genotype, the number of days to first flowering and the total number of opened flowers at the end of cultivation were recorded. For gene expression analysis, leaf disks were collected from the tip of the largest leaf of the rootstocks at ZT 15.5–16.0, at 3, 5, 7, 9, and 11 weeks after sowing of the rootstocks. Total RNA was extracted using the modified version of the Direct-TRI method as described above. Reverse transcription and RT-qPCR were performed as described above, except that the LightCycler® 96 system (Roche Diagnostics K.K., Tokyo, Japan) was used for RT-qPCR. The opened flower count and gene expression analysis were conducted only in the second replicate of the grafting experiment.

Results

Heritability of *RsFTa* expression level between two radish accessions with different graft-mediated floral induction abilities

Radish inbred line CH-IL1 is developed from a commercial pod-radish cultivar through the selection and inbreeding of individuals capable of inducing flowering in grafted cabbages (Motoki et al. 2022, Fig. 1a). Another inbred line, G2-IL1, was derived from a wild radish accession collected in Thailand, with selection focused on the early-bolting trait. In warm, LD conditions, both CH-IL1 and G2-IL1 exhibit an extremely early-bolting phenotype and do not require vernalization for flowering, with an average bolting time of 22.4 days after sowing for CH-IL1 and 28.0 days for G2-IL1 (Fig. 1b). However, when used as rootstocks, only CH-IL1 successfully induces flowering in the grafted cabbage scions, whereas G2-IL1 fails to do so (Motoki et al. 2022, Fig. 1a).

Among the two *FT* homologs reported in radish, *RsFTa* and *RsFTb* (Mitsui et al. 2023), we focused on *RsFTa*, which showed much higher expression in both G2-IL1 and CH-IL1 (Fig. S2). Expression analysis of *RsFTa* in leaves revealed that, although *RsFTa* expression was detectable in G2-IL1, CH-IL1 exhibited a markedly higher expression—95.7-fold greater on average (Fig. 1c). We first aimed to identify the genetic loci responsible for this difference in *RsFTa* expression levels through QTL analysis. In the population generated from the cross of these two accessions, the F_1 plants exhibited intermediate phenotypes relative to the parental accessions for both days to bolting and *RsFTa* expression levels (Fig. 1b, 1c). The F_2 population showed a wide range of segregation for both traits. Furthermore, a strong negative correlation was observed between these two traits in the F_2 population (Fig. S3). These results suggested that *RsFTa* expression level, which also likely contributes to the control of bolting time, is governed by multiple genetic factors.

QTL analysis for *RsFTa* expression level

We performed QTL analysis for days to bolting and *RsFTa* expression level using the F_2 population described above. A genomic library was constructed using the dpMIG-seq method (Nishimura et al. 2024), and the obtained short reads were mapped to the RS00 reference genome (Zhang et al. 2021) to identify SNPs (Table S3). Based on the genotypes of 189 F_2 individuals, a linkage map was constructed using 1,224 markers derived from 3,628 SNPs (Table S4; Data S1). QTL analysis for days to bolting (n=189) detected three QTLs with LOD peaks of 6.7, 9.1, and 49.7 located on chromosomes 3, 7, and 7, respectively (Fig. 2a). The LOD threshold for this analysis was 5.9 based on 1,000 permutations.

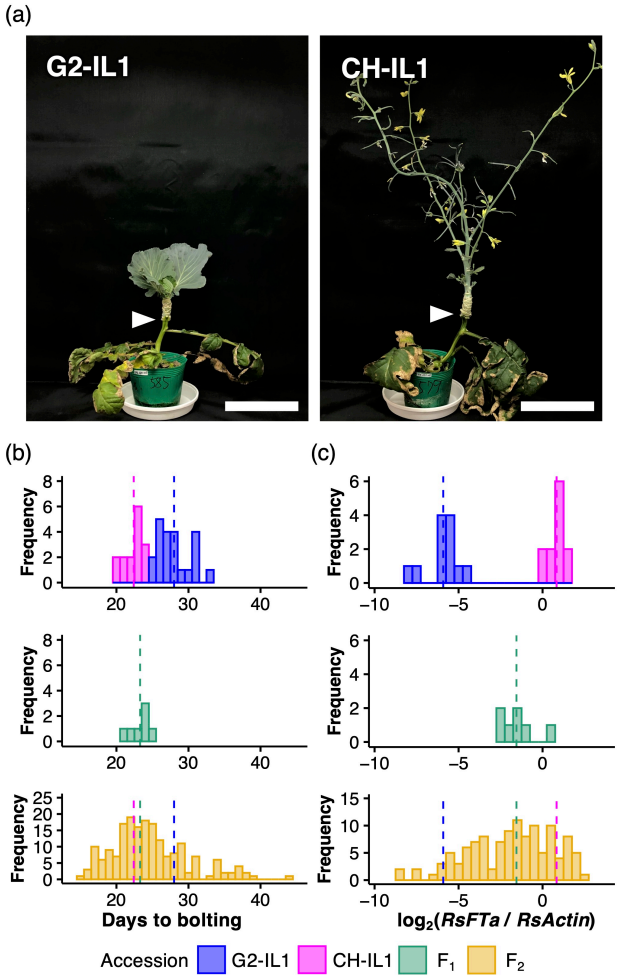

Fig. 1. Phenotype data of F_2 population and their parents showing different grafting floral induction abilities. (a) Representative pictures of cabbage scions grafted onto CH-IL1 and G2-IL1 radish rootstocks. The pictures were taken at 63 days after grafting. The cabbage grafted onto CH-IL1 started flowering while the cabbage grafted onto G2-IL1 continued vegetative growth. White arrowheads indicate graft junction. Scale bars = 10 cm. (b) A histogram of days to bolting in the radish F_1 and F_2 population and its parental accessions. (c) A histogram of the expression level of *RsFTa* in the leaf of the radish F_1 and F_2 population and its parental accessions at two weeks after sowing.

Similarly, QTL analysis for *RsFTa* expression level (n=115) identified two QTLs with LOD peaks of 12.6 and 19.0 on chromosomes 3 and 7, respectively (Fig. 2b). The LOD threshold for this analysis was 7.6 based on 1,000 permutations. Notably, the two QTLs for *RsFTa* expression level overlapped with two of the QTLs detected for days to bolting, suggesting that common genetic factors control both traits. We focused on these two QTLs affecting *RsFTa* expression and named them *qFTexp3* and *qFTexp7*, respectively. *qFTexp3* had a 1.5-LOD support interval extending from 0 to 6.6 cM, corresponding to the physical region 256,333–2,129,181 bp on chromosome 3 (Fig. 2c). *qFTexp7* had a 1.5-LOD support interval ranging from 69.6 to 73.3 cM, corresponding to 32,996,245–33,524,914 bp on chromosome 7 (Fig. 2c).

We then examined the effects of genotype combinations at *qFTexp3* and *qFTexp7* on *RsFTa* expression using the markers closest to the LOD peaks. In both QTLs, the CH-IL1 genotype increased *RsFTa* expression, and a clear interaction between the two QTLs was observed (Fig. 2d). The proportion of phenotypic variation explained by these QTLs

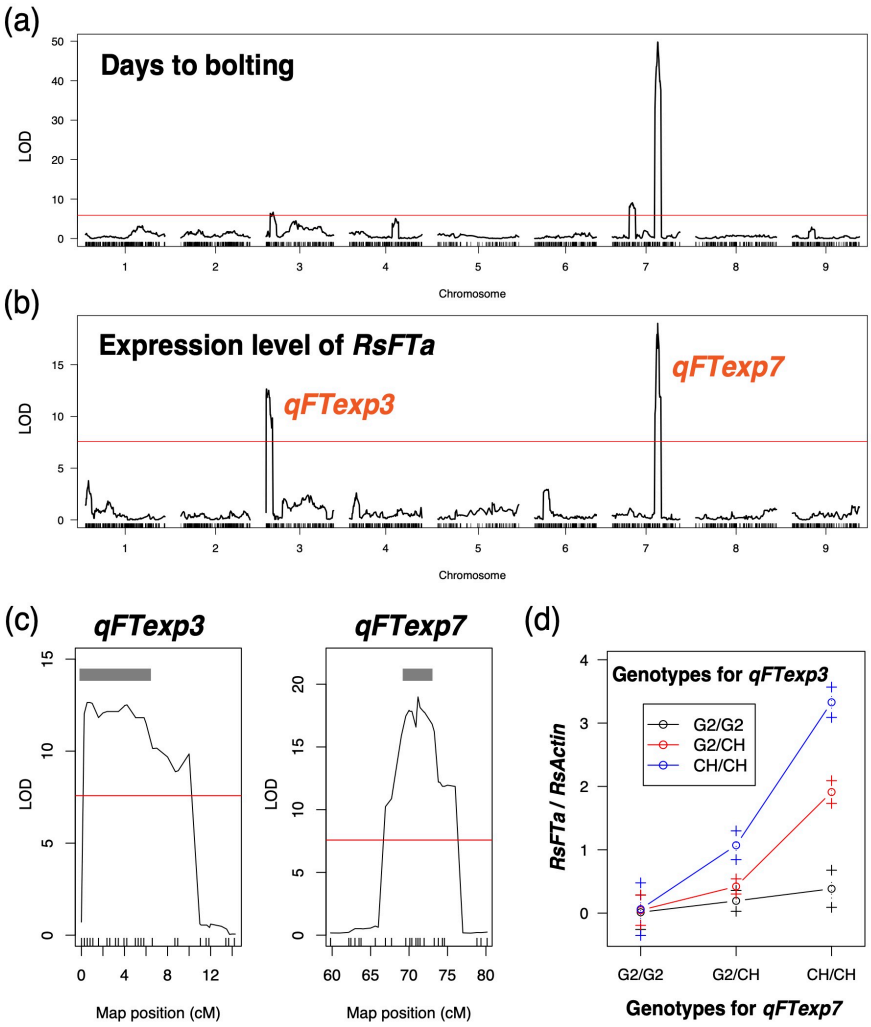

Fig. 2. The QTL analysis of the F_2 population. (a) LOD scores of QTLs for the days to bolting. (b) LOD scores of QTLs for the expression level of *RsFTa*. The red lines in (a), (b) and (c) indicate LOD score thresholds. (c) Enlarged pictures for *qFTexp3* and *qFTexp7*. The vertical lines on the x-axis show the position of markers. The gray bar shows a 1.5-LOD support interval. (d) An effect plot for the expression level of *RsFTa* in the F_2 population categorized by markers close to the LOD score peaks for *qFTexp3* and *qFTexp7*, with G2/G2, CH/CH, and G2/CH indicating the homozygous G2-IL1 allele, homozygous CH-IL1 allele, and heterozygous allele, respectively. Error bars indicate mean ± SE.

was 15.3% for *qFTexp3* and 34.9% for *qFTexp7*, indicating that *RsFTa* expression levels in the two parental accessions are predominantly controlled by these two major QTLs, with *qFTexp7* having a larger effect.

Identification of candidate genes for *qFTexp3* and *qFTexp7*

To identify candidate genes underlying *qFTexp3* and *qFTexp7*, we first performed whole-genome resequencing analysis to narrow down potential genes. Notably, the *RsFTa* gene (GWHTANWD013529) is located on chromosome 2 in the RS00 genome, outside the regions associated with these QTLs. Whole-genome resequencing of the two parental accessions revealed 1,827,287 SNPs and 597,502 indels when mapped to the RS00 reference genome. We focused on variants homozygous in both parents and annotated their functional impacts using SnpEff (Cingolani et al., 2012). In total, 98,278 SNPs and 18,335 indels were predicted to be non-synonymous. Of these, 68 and 22 non-synonymous variants were

located within the 1.5-LOD intervals of *qFTexp3* and *qFTexp7*, respectively (Fig. 3a). However, none of these variants were found in homologs of known flowering time-related genes.

Given the lack of apparent functional variants in flowering-related genes, we next investigated differential gene expression between the parental lines. RNA-seq was conducted using the largest leaves collected two weeks after sowing from G2-IL1 and CH-IL1 plants, based on the Lasy-Seq protocol (Kamitani et al., 2019; Kashima et al., 2021). A total of 1,684 upregulated genes [false discovery rate (FDR) = 0.05, $\log_2$ fold-change (FC) > 1] and 1,605 downregulated genes (FDR = 0.05, $\log_2$FC < -1) were identified in G2-IL1 (Table S5). Among these differentially expressed genes (DEGs), 64 genes were homologs of known Arabidopsis flowering-time genes (Table S5), including 15 homologs of genes that act as upstream regulators of *FT* (Fig. 3b). Notably, within the 1.5-LOD intervals of *qFTexp3* and *qFTexp7*, we identified two floral repressor genes, GWHTANWD015077 (associated with *qFTexp3* and located at 1,808,520-1,813,290 bp on chromosome 3) and GWHTANWD044743 (associated with *qFTexp7* and located at 33,049,859-33,054,708 bp on chromosome 7), which were significantly downregulated in CH-IL1 (Fig. 3a, 3b). Both genes encode homologs of *FLC*, a well-known upstream repressor of *FT* in Arabidopsis (Helliwell et al., 2006).

FLC is a MADS-box transcription factor that regulates the vernalization requirement in Arabidopsis by binding to the first intron of *FT* and repressing its expression, thereby acting as a major floral repressor (Helliwell et al., 2006; Michaels and Amasino, 1999). *FLC* homologs play key roles in the diversification of the flowering phenology in Brassicaceae family (Soppe et al. 2021) and have been repeatedly identified as major QTLs for flowering time in crops species including radish (Irwin et al. 2016; Kitamoto et al. 2014; Okazaki et al. 2007; Wang et al. 2018; Zhao et al. 2010). Radish has three copies of *FLC* homologs (*RsFLC1*, *RsFLC2*, and *RsFLC3*), and each of them was reported to function as a floral repressor in transgenic experiments (Yi et al. 2014). The reduced expression of the two *FLC* homologs in CH-IL1 was a plausible explanation for the elevated *RsFTa* expression observed in this accession. Expression levels of *RsFLC1* (GWHTANWD044743) and *RsFLC3* (GWHTANWD015077) were significantly lower in CH-IL1 compared with G2-IL1, with *RsFLC1* showing a 9.84-fold decrease and *RsFLC3* a 19.7-fold decrease (Fig. 3c). In contrast, no difference was detected in the expression of *RsFLC2*, another *FLC* homolog in the radish genome (Fig. 3c). These results suggested that *cis*-regulatory changes affecting *RsFLC1* and *RsFLC3* in CH-IL1 likely contribute to their reduced expression.

(a)

	qFTexp3	*qFTexp7*
Chr	3	7
Candidate region (1.5-LOD intervals)	256,333 - 2,129,181	32,996,245 - 33,524,914
Annotated genes in the RS00 reference genome	347	88
Flowering time-related genes (x)	5	1
DEGs (y)	50	13
Genes with HIGH or MODERATE impact mutations (z)	68	22
Flowering time-related & DEGs (x ∩ y)	**1** (GWHTANWD015077) = ***RsFLC3***	**1** (GWHTANWD044743) = ***RsFLC1***
Flowering time-related & higher impact mutation (x ∩ z)	0	0

(b)

Transcript id[z]	Chr[y]	Pos[x]	log2(G2-IL1.RPM)	log2(CH-IL1.RPM)	FDR	log2FC (CH-IL1/G2-IL1)	Gene name[w]
GWHTANWD015077	3	1,808,520	6.4	2.0	2.E-08	-4.3	***FLC***
GWHTANWD044743	7	33,049,859	6.7	3.4	4.E-06	-3.3	***FLC***
GWHTANWD009802	2	6,986,977	-0.2	2.9	3.E-05	3.1	*EBS*
GWHTANWD024596	4	37,881,482	2.6	0.0	1.E-04	-2.6	*CDF2*
GWHTANWD000760	1	3,554,621	0.9	3.1	2.E-04	2.3	*NF-YB1*
GWHTANWD000759	1	3,554,621	1.2	3.1	1.E-03	2.0	*NF-YB1*
GWHTANWD012086	2	18,287,669	0.5	2.4	2.E-03	2.0	*TOE2*
GWHTANWD000761	1	3,554,640	1.3	2.6	1.E-02	1.3	*NF-YB1*
GWHTANWD045156	7	34,802,023	1.2	3.7	3.E-05	2.5	*CO*
GWHTANWD055397	9	42,422,586	2.3	-1.4	5.E-04	-3.5	*COL5*
GWHTANWD050723	8	37,272,249	2.3	0.5	1.E-03	-1.8	*STO*
GWHTANWD039978	6	42,904,393	3.9	4.9	1.E-03	1.1	*CRY2*
GWHTANWD016710	3	9,476,759	4.3	2.8	5.E-03	-1.5	*SPL3*
GWHTANWD039810	6	42,234,636	4.1	2.2	8.E-03	-1.9	*STO*
GWHTANWD049706	8	33,028,613	1.9	3.0	3.E-02	1.2	*PFT1*

(c)

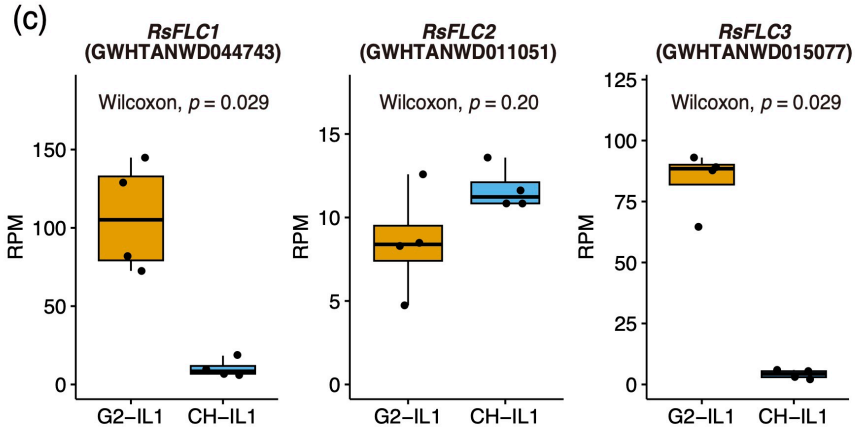

Fig. 3. Identification of the candidate genes for *qFTexp3* and *qFTexp7* by RNA-seq analysis and whole genome re-sequence analysis. (a) Integration of QTL analysis, RNA-seq analysis and whole genome re-sequence analysis for *qFTexp3* and *qFTexp7*. * Number of genes with polymorphisms between G2-IL1 and CH-IL1 which were annotated as HIGH or MODERATE for impact in SnpEff analysis of whole genome resequencing data. (b) List of differentially expressed genes (DEGs) between G2-IL1 and CH-IL1 that are predicted to be homologs of upstream regulator genes of *FT* in Arabidopsis (FDR = 0.05). The blue heatmap in the upper panel and the red heatmap in the lower panel indicate the homologs of genes with negative and positive effects on expression of *FT* in Arabidopsis, respectively. [z]Transcript id is the name of the transcript in the RS00 reference genome. [y]Chr shows chromosome. [x]Pos indicates the transcription start site for each gene in the RS00 reference genome. [w]Gene name indicates the Arabidopsis gene with the highest homology. (c) Expression level of the three *FLC* homologs in the RNA-seq data. The results of the Wilcoxon test between G2-IL1 and CH-IL1 are shown in the graph (n=4).

348

Characterization of the genomic sequences of *RsFLC1* and *RsFLC3*

To investigate allelic variation in *RsFLC1* and *RsFLC3* between G2-IL1 and CH-IL1 and to identify potential *cis*-regulatory elements responsible for the reduced expression in CH-IL1, we first searched the radish pangenome (Zhang et al., 2021) for reference genomes with the highest sequence similarity to the *RsFLC1* and *RsFLC3* regions. Short reads from both parental accessions were mapped to the 11 reference genomes constituting the pangenome, and the number of homozygous variants within the open reading frames (ORFs) of *RsFLC1* and *RsFLC3* was calculated. For *RsFLC1*, G2-IL1 showed the highest similarity to RS00 (*R. sativus* var. *longipinnatus*), whereas CH-IL1 was most similar to RS08 (*R. raphanistrum* ssp. *landra*), as indicated by the lowest number of detected variants (Fig. 4a). For *RsFLC3*, G2-IL1 showed the highest similarity to RS03 (*R. sativus* var. *niger*), whereas CH-IL1 was most similar to RS09 (*R. raphanistrum* ssp. *raphanistrum*) (Fig. 4b).

Next, we extracted genomic regions containing *RsFLC1* and *RsFLC3*, along with their flanking sequences, from the respective reference genomes to compare gene structures and identify potential structural variations. In *RsFLC1*, we identified a large inverted repeat of approximately 10 kb in the RS08 genome (Fig. S4a, Fig. 4c). This sequence, spanning the promoter region and exons 1 to 6 of the RS00 *RsFLC1* gene, was inserted between exons 6 and 7 of the RS00 gene model. Although this structural variant could not be amplified by PCR, Oxford Nanopore long-read sequencing of CH-IL1 confirmed its presence by capturing reads spanning the entire region (Fig. S5). For *RsFLC3*, no large structural variations were detected, unlike in *RsFLC1*. However, three indels were identified in the RS09 genome, the closest reference to CH-IL1: a 713-bp insertion in the first intron, a 585-bp deletion in the ninth intron, and another 1176-bp deletion in downstream of the gene (Fig. S4b, Fig. 4d).

To identify potential *cis*-regulatory variation underlying the differences in *RsFLC1* and *RsFLC3* expression between alleles, we examined polymorphisms in the promoter regions of these genes. In *A. thaliana*, the 272-bp region upstream of the start codon has been identified as the minimal promoter required for *FLC* expression prior to vernalization (Sheldon et al. 2002). This region contains ABA-responsive *cis*-regulatory elements (ABREs) known to be involved in the upregulation of *FLC* expression in response to abscisic acid (Xu et al. 2022). In addition, a SUF4-binding motif has been identified upstream of the minimal promoter, which is bound by SUF4, a component of the FRIGIDA complex that enhances *FLC* transcription (Choi et al. 2011). In *RsFLC1*, we identified one ABRE-like motif (shared by *AtFLC* and *RsFLC1*: ACACGTGGC) and one SUF4 binding motif-like sequence (*AtFLC*: CCAAATTTTAAGTTT; *RsFLC1*: AGAAATTCAAAGTAT) within 400 bp upstream of the start codon (Fig. 4e). Although three SNPs were found between the G2-IL1 and CH-IL1 alleles in the region homologous to the minimal promoter, none overlapped with the identified motifs. Thus, no promoter mutations were found that clearly disrupt known regulatory elements. Given this, it is possible that the large intragenic inversion identified in *RsFLC1*—which spans the promoter and early exons—rather than specific *cis*-regulatory sequence changes, may underlie the loss of expression observed in CH-IL1. In contrast, the *RsFLC3* promoter exhibited more extensive sequence variation (Fig. 4f). Within the 500-bp upstream region of the start codon, we identified one ABRE-like motif (ACACGTGGC) and one SUF4 binding motif-like sequence (ACAAATTTTTAGTAT) in the G2-IL1 allele, both of which harbored SNPs in CH-IL1 allele (ACATGTGGC in the ABRE-like motif and

(a) *RsFLC1*

Reference genome	Species	Transcript ID	G2-IL1 SNPs	G2-IL1 Indels	G2-IL1 Total	CH-IL1 SNPs	CH-IL1 Indels	CH-IL1 Total
RS00	***R. sativus* var. *longipinnatus***	GWHTANWD044743	**0**	**0**	**0**	16	11	27
RS01	*R. sativus* var. *caudatus*	GWHTANWE039208	18	11	29	22	14	36
RS02	*R. sativus* var. *oleiformis*	GWHTANWJ044734	18	7	25	17	9	26
RS03	*R. sativus* var. *niger*	GWHTANWK040362	3	2	5	11	5	16
RS04	*R. sativus* var. *longipinnatus*	GWHTANWR036961	6	10	16	15	14	29
RS05	*R. sativus* var. *longipinnatus*	GWHTANWQ039927	11	8	19	16	13	29
RS06	*R. sativus* var. *radicula*	GWHTANWP039945	22	14	36	22	18	40
RS07	*R. sativus* var. *raphanistroides*	GWHTANWS039425	30	15	45	29	18	47
RS08	***R. raphanistrum* ssp. *Landra***	GWHTANWL036592	19	9	28	**4**	**2**	**6**
RS09	*R. raphanistrum* ssp. *Raphanistrum*	GWHTANWM033513	162	29	191	138	29	167
RS10	*R. raphanistrum* × *R. sativus*	GWHTANWN040610	12	9	21	17	14	31

(b) *RsFLC3*

Reference genome	Species	Transcript ID	G2-IL1 SNPs	G2-IL1 Indels	G2-IL1 Total	CH-IL1 SNPs	CH-IL1 Indels	CH-IL1 Total
RS00	*R. sativus* var. *longipinnatus*	GWHTANWD015077	6	4	10	112	19	131
RS01	*R. sativus* var. *caudatus*	GWHTANWE013758	95	12	107	3	3	6
RS02	*R. sativus* var. *oleiformis*	GWHTANWJ013050	1	2	3	40	6	46
RS03	***R. sativus* var. *niger***	GWHTANWK012587	**0**	**0**	**0**	99	10	109
RS04	*R. sativus* var. *longipinnatus*	GWHTANWR012296	1	3	4	94	16	110
RS05	*R. sativus* var. *longipinnatus*	GWHTANWQ012445	1	3	4	94	15	109
RS06	*R. sativus* var. *radicula*	GWHTANWP012343	110	21	131	78	17	95
RS07	*R. sativus* var. *raphanistroides*	GWHTANWS012468	95	13	108	3	4	7
RS08	*R. raphanistrum* ssp. *Landra*	GWHTANWL013047	108	12	120	15	3	18
RS09	***R. raphanistrum* ssp. *Raphanistrum***	GWHTANWM010824	95	11	106	**0**	**1**	**1**
RS10	*R. raphanistrum* × *R. sativus*	GWHTANWN012258	95	13	108	3	4	7

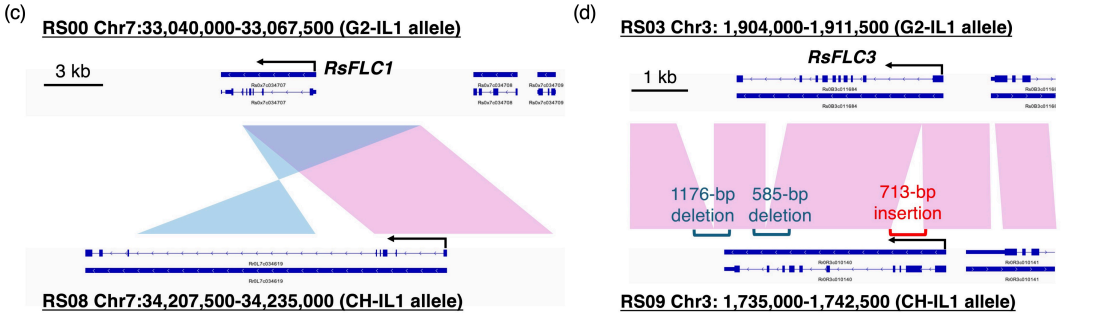

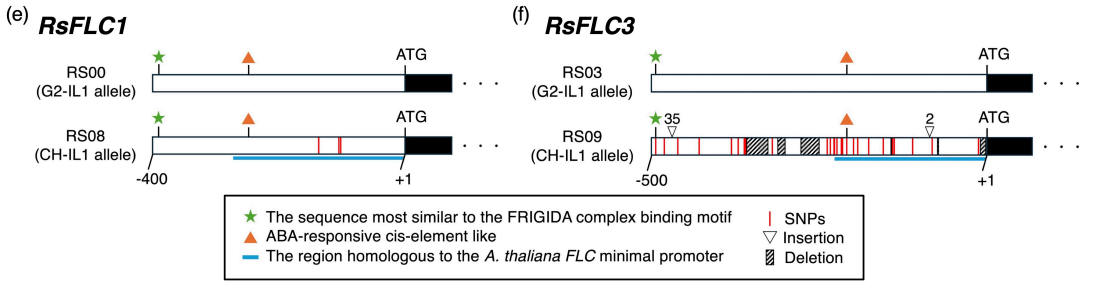

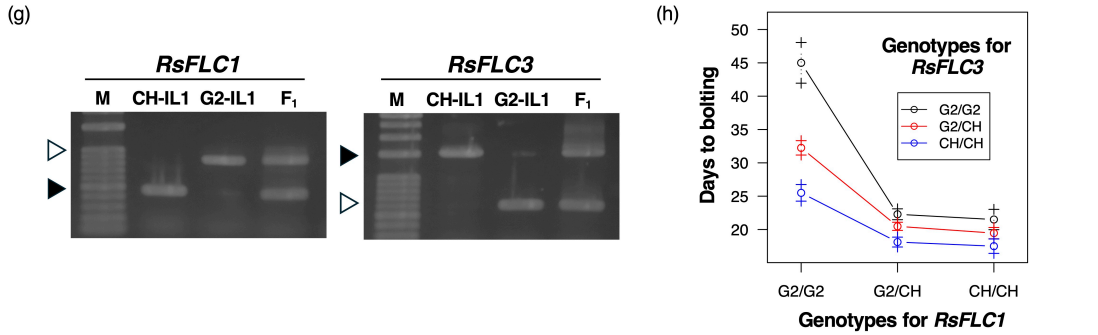

Fig. 4. Characterization of genomic sequences of *RsFLC1* and *RsFLC3*. (a, b) Number of homozygous polymorphisms against 11 radish reference genomes within the open reading frame (ORF) of *RsFLC1* (a) and *RsFLC3* (b) in the whole genome resequencing data. Orange shading indicates the lowest number of polymorphisms in each accession. (c, d) Analysis of structural variations around *RsFLC1* (c) and *RsFLC3* (d) between the most similar reference genomes for G2-IL1 and CH-IL1. The syntenic relationships between the two genomes are visualized based on the dot plot analysis. For simplicity, small structural variations are omitted in (c). The gene models in the corresponding regions are visualized based on the GFF files of each reference genome using Integrative Genomics Viewer. (e, f) Polymorphisms in the promoter regions of *RsFLC1* (e) and *RsFLC3* (f) between G2-IL1 and CH-IL1 alleles. (g) Electrophoresis images of the amplified products by multi-plex PCR using the primer sets shown in Fig. S1 for *RsFLC1* and *RsFLC3*, respectively. White and black arrowheads indicate the amplicon size expected from G2-IL1 and CH-IL1 allele, respectively. (h) An effect plot for the days to bolting in the F_3 population categorized by the above mentioned primer sets for *RsFLC1* and *RsFLC3*, with G2/G2, CH/CH, and G2/CH indicating the homozygous G2-IL1 allele, homozygous CH-IL1 allele, and heterozygous allele, respectively. Error bars indicate mean ± SE.

ACAAAATTTTAGTAT in the SUF4-binding motif-like sequence). In addition to these motif-level changes, numerous SNPs and indels were found across the *RsFLC3* promoter region, suggesting the *cis*-regulatory divergence that may contribute to the differential gene expression between alleles. In this study, we did not further experimentally validate which *cis*-regulatory variants underlie the loss-of-expression phenotype; this remains to be elucidated through future functional analyses.

Based on the structural variants described above, we developed allele specific markers that discriminated the G2-IL1 and CH-IL1 alleles (Fig. 4g, Fig. S1). Using these markers, we genotyped 96 F_3 individuals grown under natural LD conditions in a greenhouse and analyzed the relationship between genotype and days to bolting as a proxy for *RsFTa* expression. The results showed that these allele-specific markers were significantly associated with flowering time in the F_3 population (Fig. 4h), confirming the effect of the CH-IL1 alleles. We named these previously unreported loss-of-expression *FLC* alleles from CH-IL1 as $rsflc1^{Ldr1}$ and $rsflc3^{Rpn1}$, and the functional *FLC* alleles from G2-IL1 as $RsFLC1^{Lpt1}$ and $RsFLC3^{Ngr1}$, based on their corresponding reference genomes.

Combinatorial effects of *RsFLC1* and *RsFLC3* alleles on graft-mediated floral induction ability in radish rootstocks

We next investigated whether the loss-of-expression *FLC* alleles identified in this study enhanced graft-mediated floral induction ability in radish rootstocks. From the F_2 population derived from the G2-IL1 × CH-IL1 cross, we selected individuals homozygous at both *RsFLC1* and *RsFLC3* loci using the allele-specific markers. Four genotypic combinations were analyzed: $RsFLC1^{Lpt1}/RsFLC3^{Ngr1}$, $RsFLC1^{Lpt1}/rsflc3^{Rpn1}$, $rsflc1^{Ldr}/RsFLC3^{Ngr1}$, and $rsflc1^{Ldr}/rsflc3^{Rpn1}$ (7–10 individuals per combination). These plants were grown under LD conditions, and cabbage seedlings were grafted onto their floral stems at the time of bolting.

In the radish rootstocks themselves, $rsflc1^{Ldr1}$ significantly accelerated bolting (about 10 days earlier than $RsFLC1^{Lpt1}$), whereas the *RsFLC3* genotype had little effect (Fig. 5a). Leaf area of the rootstocks at grafting was positively correlated with bolting time; $rsflc1^{Ldr1}$ genotypes developed smaller leaves than $RsFLC1^{Lpt1}$ (Fig. 5b). Time-course gene expression analysis in the rootstock leaves showed that the overall tendency of *RsFTa* levels followed the order: $rsflc1^{Ldr1}/RsFLC3^{Ngr1} > rsflc1^{Ldr1}/rsflc3^{Rpn1} > RsFLC1^{Lpt1}/rsflc3^{Rpn1} > RsFLC1^{Lpt1}/RsFLC3^{Ngr1}$ (Fig. 5c), although at 3 weeks after sowing, $rsflc1^{Ldr1}/rsflc3^{Rpn1}$ showed the highest expression levels. Expression levels were consistently higher in $rsflc1^{Ldr1}$ genotypes from 5 weeks after sowing onward. $rsflc3^{Rpn1}$ showed limited effects depending on the *RsFLC1* background: increased expression was observed at early stages in the $rsflc1^{Ldr1}$ background and at later stages in the $RsFLC1^{Lpt1}$ background, relative to $RsFLC3^{Ngr1}$ genotypes. Regarding the expression of the *FLC* homologs themselves, both $rsflc1^{Ldr1}$ and $rsflc3^{Rpn1}$ showed similarly negligible expression, as expected (Figs. 5d, 5e). In contrast, the functional alleles exhibited distinct expression dynamics: $RsFLC1^{Lpt1}$ was stably and highly expressed throughout the growth period, whereas $RsFLC3^{Ngr1}$ showed unstable and gradually declining expression, particularly in the $rsflc1^{Ldr1}$ background.

The flowering response of grafted cabbage scions were clearly affected by rootstock genotypes (Figs. 5f–h). Nearly all scions grafted onto rootstocks with $rsflc1^{Ldr1}$ genotype flowered. In contrast, flowering occurred at a lower frequency in $RsFLC1^{Lpt1}$ genotypes—particularly in the $RsFLC1^{Lpt1}/RsFLC3^{Ngr1}$ combination, where only 1 out of 8 scions

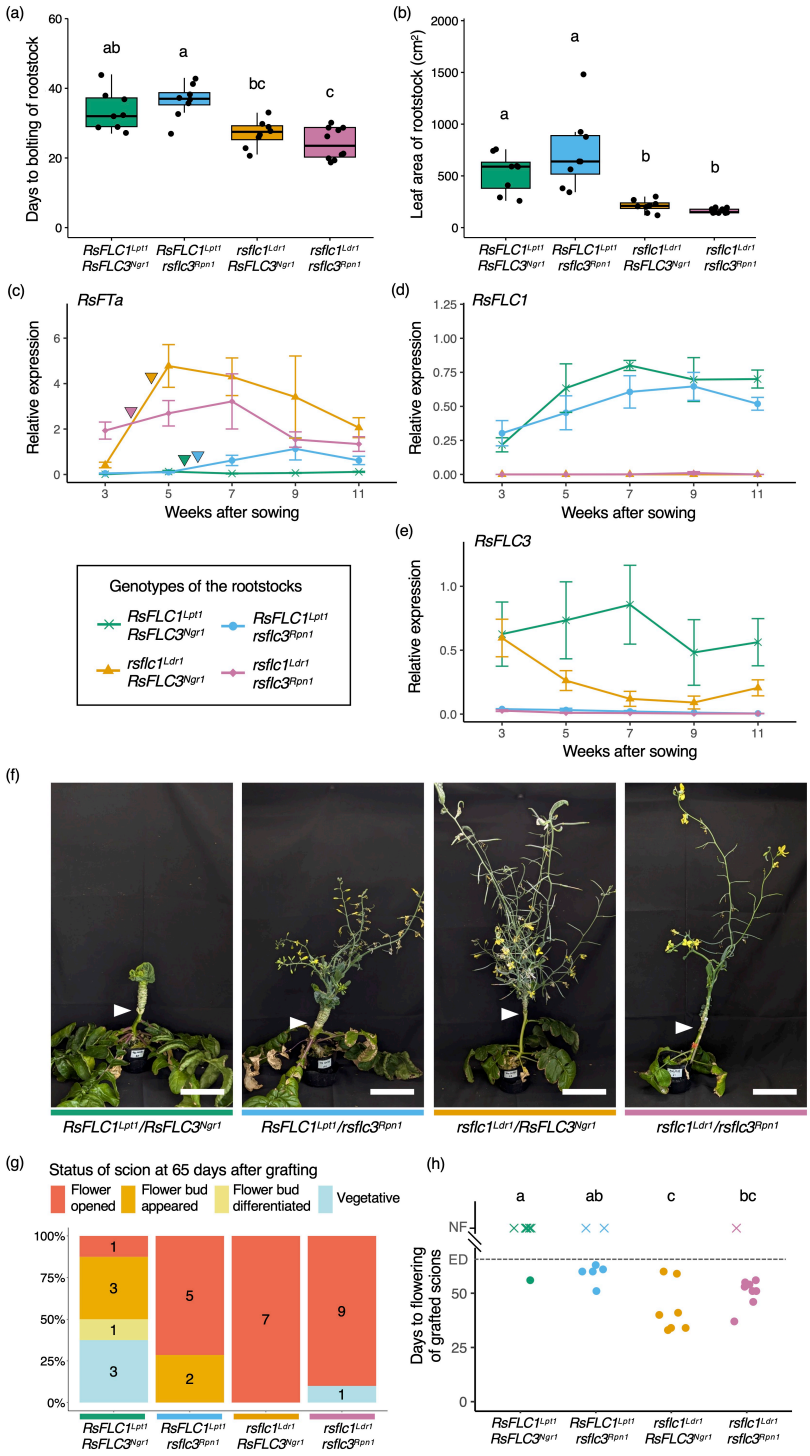

Fig. 5. Effect of *RsFLC1* and *RsFLC3* alleles on the floral induction ability of radish rootstocks. (a) Days to bolting after sowing of the radish rootstocks themselves. (b) Total area of leaves left on rootstocks after grafting at the day of grafting. (c–e) Time-course gene expression of (c) *RsFTa*, (d) *RsFLC1*, and (e) *RsFLC3* in the leaves of radish rootstocks used for the grafting experiment. At each time point, leaf disks were sampled from the largest non-yellowing leaves of each rootstock plant. *RsActin* was used as an internal control. Error bars indicate mean ± SE (n = 4–5). Arrowheads in the *RsFTa* graph indicate the average time point of grafting for each rootstock genotype. (f) Representative pictures of cabbage scions grafted onto F_2 individuals with different combination of *RsFLC1* and *RsFLC3* alleles. The pictures were taken at 65 days after grafting. White arrowheads indicate graft junction. Scale bars = 10 cm. (g) Floral status of the grafted scions at 65 days after grafting. (h) Days to flowering after grafting of the cabbage grafted onto F_2 individuals. ED: end of experiment; NF: non-flowering. Different letters indicate statistical difference among the treatments with pairwise Wilcoxon tests with the Bonferroni adjustment for multiple comparisons ($P < 0.05$, n = 7–10) in (a), (b) and (h).

flowered (Fig. 5g). *rsflc1*^{Ldr1} also led to earlier flowering and more opened flowers (Fig. 5h, Fig. S6). *rsflc3*^{Rpn1} improved floral induction only in the *RsFLC1*^{Lpt1} background (Figs. 5g, 5h). These findings demonstrated that *rsflc1*^{Ldr1}, a major-effect allele for *RsFTa* upregulation, strongly promoted graft-mediated floral induction. In contrast, *rsflc3*^{Rpn1}, a minor-effect allele, enhanced graft-mediated floral induction only in the presence of a functional *RsFLC1* allele.

Distribution of *FLC* loss-of-expression alleles in radish germplasm

To investigate the origin of the loss-of-expression *FLC* alleles identified in CH-IL1, we surveyed a panel of *Raphanus* accessions (Table S1). Pangenome analysis showed that the *rsflc1*^{Ldr1} and *rsflc3*^{Rpn1} alleles were most similar to RS08 and RS09 reference genomes, which were derived from *R. raphanistrum*, a weedy radish species (Figs. 4a, 4b). Genotyping of diverse *R. sativus* and *R. raphanistrum* accessions revealed that the *rsflc1*^{Ldr1} allele was exclusive to *R. raphanistrum*, and the *rsflc3*^{Rpn1} allele was detected in both species, although it was much less frequent in *R. sativus* (Fig. 6a; Table S1). All three accessions carrying the *rsflc1*^{Ldr1} allele were collected from the United States (Table S1). The *rsflc3*^{Rpn1} allele was found in accessions originating from five different countries, suggesting a broader geographic distribution. Furthermore, both the *rsflc1*^{Ldr1} and *rsflc3*^{Rpn1} alleles were present in a heterozygous state in each of these accessions (Table S1), as well as in the original cultivar used to develop the CH-IL1 inbred line (Fig. 6b).

(a)

Species	Subspecies / Variety	n	Accessions possessing *rsflc1*^{Ldr1}	Accessions possessing *rsflc3*^{Rpn1}
Raphanus sativus	var. *hortensis*	76	0	0
	var. *caudatus*	13	0	0
	var. *niger*	1	0	**1**
	var. *sativus*	19	0	**2**
	var. *raphanistroides*	2	0	0
	unknown	15	0	**1**
Raphanus raphanistrum	ssp. *maritimus*	4	0	**3**
	ssp. *landra*	3	**1**	0
	unknown	3	**2**	**1**

(b)

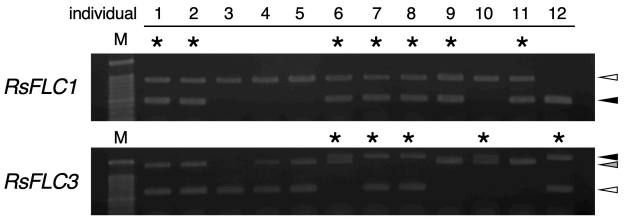

Fig. 6. Distribution of *FLC* loss-of-expression alleles in radish germplasm. (a) Summary of the genotyping of diverse *R. sativus* and *R. raphanistrum* accessions. (b) Heterozygous state of *FLC* loss-of-expression alleles in the original cultivar used to develop CH-IL1. Black arrowheads indicate the bands corresponding to *rsflc1*^{Ldrl} and *rsflc3*^{Rpnl} alleles, and white arrowheads indicate the bands corresponding to *RsFLC1*^{Lptl} and *RsFLC3*^{Ngr1}. The smaller bands in the *RsFLC3* result, indicated by gray arrowheads, represent amplicons derived from an allele type other than *rsflc3*^{Rpnl} or *RsFLC3*^{Ngr1}. Asterisks indicate individuals carrying heterozygous loss-of-expression *FLC* alleles.

Discussion

Natural variations underlying differences in graft-mediated floral induction ability

In this study, we identified two unreported loss-of-expression alleles of *FLC* as QTLs that enhanced *FT* expression in radish, and showed that these alleles contributed to the variation in the graft-mediated floral induction. Although previous studies reported that the genotype of rootstocks affected quantitative differences in graft-mediated floral induction (Fujise et al. 1964; Motoki et al. 2022), this study is the first report identifying the underlying genetic factors responsible for such differences. Rootstocks possessing the functional *FLC* alleles used in this study flowered early under non-vernalized conditions (Fig. 5a). However, they were much less effective and exhibited unstable floral induction of grafted cabbage scions (Figs. 5f–h). This suggested that flowering of the rootstock itself is not sufficient to trigger the graft-mediated floral induction in the scion, which aligns with previous findings (Motoki et al. 2022; Putterill and Varkonyi-Gasic 2016; Tang et al. 2022; van de Pol 1972).

Based on these observations, we propose a model for successful graft-mediated floral induction using radish rootstocks (Fig. 7). At high levels of *FLC* expression, *FT* expression is strongly repressed, and neither the radish rootstock itself nor the grafted cabbage scion does not flower (Fig. 7a). As *FLC* expression decreases, *FT* expression is initiated, triggering flowering in the rootstock. However, this level of *FT* is insufficient to induce flowering in grafted scions (Fig. 7b). A further decrease in *FLC* expression leads to higher *FT* expression, which enables floral induction in the scion (Fig. 7c). The underlying mechanism behind the different *FT* thresholds required for flowering in rootstocks and scions remains unclear. Possible explanations include differences in sensitivity of meristems to FT between rootstocks and scions or limited FT transmission across the graft junction. As a future work, it will be of interest to examine whether this model can

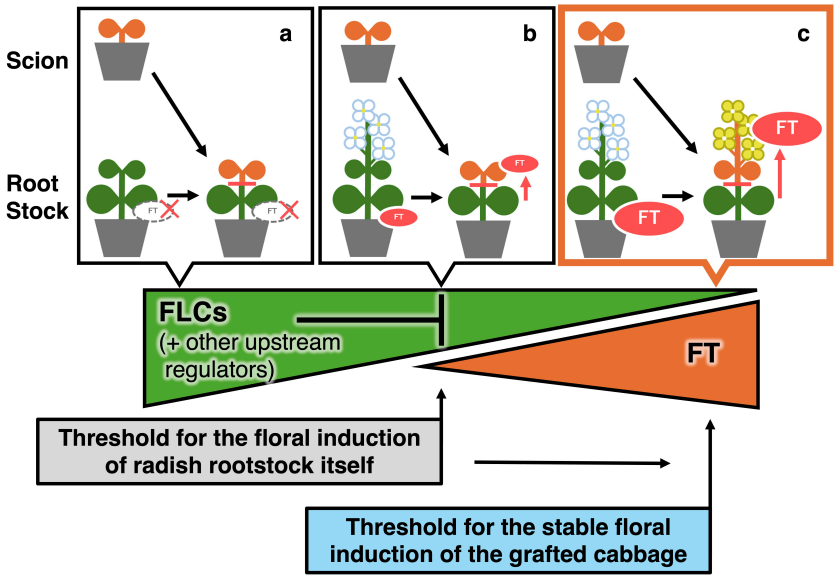

Fig. 7. A proposed model for successful graft-mediated floral induction using radish rootstocks. (a) At high levels of *FLC* expression, *FT* expression is strongly repressed, and neither the radish rootstock nor the grafted cabbage scion undergoes flowering. (b) A moderate reduction in *FLC* expression initiates *FT* expression, enabling flowering of the rootstock itself; however, this *FT* level remains insufficient to stably induce flowering in the grafted cabbage scion. (c) A further reduction in *FLC* expression results in a substantial increase in *FT* expression, which exceeds the threshold required to reliably induce flowering in the scion. This model implies that natural variation in other upstream regulators of *FT* may also influence the stability of graft-mediated floral induction.

also explain inter-specific variations in graft-mediated floral induction ability, as observed between *R. sativus* and *B. oleracea* rootstocks (Kagawa 1957; Motoki et al. 2019, 2022).

While *FLC* is a major upstream regulator of *FT* in Arabidopsis, several other transcription factors regulate *FT* expression in parallel with *FLC* (Kinoshita and Richter 2020). Additionally, mutations in the *cis*-regulatory regions of the *FT* locus itself alter its gene expression level (Liu et al. 2014), although in this study no expression QTLs for *RsFTa* were detected on chromosome 2, where *RsFTa* gene is located (Fig. 2b). Therefore, by searching a broader range of radish germplasm, natural variations that enhance *FT* expression, other than the variations in *FLC*, may be identified as additional genetic factors for promoting graft-mediated floral induction. In the closely related species *B. rapa,* an accession carrying a mutated *FT* allele with increased expression level was reported to induce flowering in grafted radish scions (Nishikawa et al. 2023), supporting this possibility.

Differential effects of *RsFLC1* and *RsFLC3* alleles on *RsFTa* expression and graft-mediated floral induction ability

Both loss-of-expression *FLC* alleles identified in this study showed little to no expression throughout the growth period (Figs. 5d, 5e). However, $rsflc1^{Ldr1}$ had a stronger effect than $rsflc3^{Rpn1}$ on both *RsFTa* expression in the rootstock and its graft-mediated floral induction ability (Figs. 5c, 5f, 5g). One possible explanation for this difference lies in the expression patterns of their corresponding functional alleles: $RsFLC1^{Lpt1}$ maintained high expression throughout the growth period, whereas $RsFLC3^{Ngr1}$ exhibited weaker and unstable expression that declined over time (Figs. 5d, 5e). Previous studies have reported that variations in expression levels of *FLC* homologs are associated with their floral repression activity in several *Brassica* species (Calderwood et al. 2021; Hepworth et al. 2020; Kinoshita et al. 2023; Kitamoto et al. 2014; Wang et al. 2018). Therefore, the instability of $RsFLC3^{Ngr1}$ expression was suggested to cause a smaller phenotypic contrast with its loss-of-expression counterpart. In line with this hypothesis, at early growth stage (3 weeks after sowing) when *RsFLC3* expression remains high in the $rsflc1^{Ldr1}/RsFLC3^{Ngr1}$ genotype, *RsFTa* expression was higher in $rsflc1^{Ldr1}/rsflc3^{Rpn1}$ than $rsflc1^{Ldr1}/RsFLC3^{Ngr1}$ (Fig. 5c).

At 5 weeks after sowing, *RsFTa* expression became higher in $rsflc1^{Ldr1}/RsFLC3^{Ngr1}$ than in $rsflc1^{Ldr1}/rsflc3^{Rpn1}$ (Fig. 5c). This increase cannot be explained solely by the expression difference between *RsFLC1* and *RsFLC3*, since *RsFLC3* expression was still detected at relatively higher levels in $rsflc1^{Ldr1}/RsFLC3^{Ngr1}$ at this stage. Instead, it may reflect the influence of other factors such as plant size: $rsflc1^{Ldr1}/RsFLC3^{Ngr1}$ plants exhibited slightly delayed bolting and developed larger leaves compared to $rsflc1^{Ldr1}/rsflc3^{Rpn1}$ (Figs. 5a, 5b). Because *FT* expression is known to be affected by developmental stage (Castillejo and Pelaz 2008) and carbohydrate signaling in Arabidopsis (King et al. 2008; Wahl et al. 2013), the elevated *RsFTa* expression may be attributable to advanced developmental stage or enhanced carbohydrate signaling linked to the larger plant size.

Besides transcriptional differences, amino acid differences between *RsFLC1* and *RsFLC3* may contribute to their functional divergence, which was not investigated in this study. Further investigation into the molecular and functional differences between these two homologs may provide valuable insights into the regulation of flowering in radish.

Evolutionary origin and maintenance of loss-of-expression *FLC* alleles in radish

Building on our genomic and germplasm analyses, we inferred that both loss-of-expression *FLC* alleles originated from *R. raphanistrum*, a weedy radish species (Figs. 4a, 4b, 6a). *R. raphanistrum* is a globally distributed noxious weed (Kebaso et al. 2020), and early flowering has been reported as an adaptive trait enhancing seed dispersal in disturbed conditions (Ashworth et al. 2016; Charbonneau et al. 2018). Experimental evolution and modeling studies suggested that flowering time variation in *R. raphanistrum* can be explained by the presence of a major-effect gene and a minor-effect gene (Somerville et al. 2024). The two loss-of-expression *FLC* alleles identified in this study were strongly associated with early flowering (Figs. 2a, 4h), suggesting that they represent a part of the genetic basis for early flowering in *R. raphanistrum*. Recently, Li et al. (2023) reported that the mutations in *FLC* contribute to early flowering and adaptation in another Brassicaceae weed, *Cardamine occulta*, and suggested a common evolutionary trajectory of early flowering in ruderal weeds in Brassicaceae. Our results provide another example supporting this hypothesis.

CH-IL1, the accession used in our genetic analysis, was derived from a commercial *R. sativus* var. *caudatus* (pod radish) cultivar through selection for high *RsFTa* expression and ability to induce flowering in grafted scions (Motoki et al., 2022). However, surveys of genetic resources revealed that the *rsflc1*^{Ldr1} and *rsflc3*^{Rpn1} alleles are absent from other *R. sativus* var. *caudatus* accessions (Table S1). Further analysis showed that these alleles were present in a heterozygous state in the original seeds from which CH-IL1 is derived (Fig. 6b). Taken together, these findings imply that the loss-of-expression *FLC* alleles have introgressed from *R. raphanistrum*, which was possibly present in or near the commercial seed production site, into the pod radish cultivar through unintentional hybridization during seed multiplication.

Application of identified natural variation in breeding of florigenic rootstocks and conventional root-type radish

The allele-specific markers developed for the loss-of-expression *FLC* alleles enable efficient breeding of radish rootstocks with enhanced graft-mediated floral induction ability. Previous studies have shown that not only *FT* mRNA expression levels, but also the amount of leaves—where FT is produced— in rootstocks are key determinants of graft-mediated floral induction (Motoki et al., 2022; Suge 1984; Zeevaart 1958). For instance, introducing these alleles into radish accessions with larger or longer-lived leaves will help generate rootstocks with even greater florigenic potential. Additionally, combining these alleles with disease resistance traits may facilitate the development of robust rootstocks suited to diverse breeding environments.

Beyond rootstocks for grafting, these markers are also valuable in breeding programs for conventional root-type radish cultivars. As *R. raphanistrum* is cross-compatible with cultivated radish, it serves as a useful genetic resource for expanding the gene pool. For example, it was shown that herbicide resistance can be introduced from *R. raphanistrum* to *R. sativus*, which can lead to the development of herbicide-tolerant cultivars (Jugulam et al. 2014). However, the early bolting trait associated with *R. raphanistrum* may compromise root development in cultivars bred for root harvest. The molecular markers developed in this study can support the effective elimination of undesirable early bolting alleles while preserving key traits of *R. raphanistrum*.

Conclusion: A strategy for developing florigenic rootstocks for floral induction in other crops

In this study, we identified naturally occurring loss-of-expression *FLC* alleles in radish as key genetic variations underlying enhanced graft-mediated floral induction ability, through increased *FT* gene expression levels. Our findings suggest that initial screening based on *FT* expression levels serves as a practical approach to efficiently develop highly florigenic rootstocks. Importantly, we found that the loss-of-expression *FLC* alleles originated from *R. raphanistrum*, a weedy species adapted to disturbed environments through early flowering. This finding highlights the importance of exploring genetic diversity in wild and weedy relatives, in addition to cultivated germplasm, for identifying naturally occurring alleles that confer high *FT* expression and enhance floral induction. Our study experimentally demonstrates that graft-mediated floral induction can be enhanced by genetic improvement of *FT* expression levels in the rootstocks, thus providing a framework for developing florigenic rootstocks that may facilitate the application of graft-mediated floral induction in other crops.

Statements and Declarations

Funding

This work was supported by Japan Society for the Promotion of Science (JSPS) [KAKENHI Grant-in-Aid for JSPS Fellows 19J15038, Grant-in-Aid for Young Scientists（B） 20K15518 and 23K13943].

Competing Interests

The findings described in this manuscript are included in a Japanese patent application (application number: JP2025-151145 in Japan) related to the use of radish rootstocks for graft-mediated floral induction. KM, SK, KN, YK and MH are listed as applicants on this patent. The authors declare that there are no other potential conflicts of interest.

Data Availability

All sequence data have been deposited in the DDBJ database. The corresponding accession numbers are listed below, and additional details for individual samples are provided in the Table S6. The DRA accession numbers assigned are PRJDB35551, PRJDB35552, PRJDB35582 and PRJDB35583. The plant materials and datasets used in this study will be available by the corresponding author upon request.

Author Contributions

Conceptualization: KM, YK, MH; Data curation: KM, SK, KN, MK, KU; Formal analysis: KM, KN, YK, MK, KU; Funding acquisition: KM; Investigation: KM, SK, KN, MK, KU; Methodology: KM, KN, YK, MK, KU; Project administration: KM; Resources: KM, KN, MK, KU, TG, KY, MH; Software: KN, MK; Supervision: KM, YK, TG, KY, MH; Validation: KM, SK, YK; Visualization: KM, SK, KN, YK, KU; Writing – original draft: KM, SK, YK, – review & editing: KN, MK, KU, TG, KY, MH.

Short legends for Supporting Information

Fig. S1 Design of allele-specific markers for *RsFLC1* and *RsFLC3* of G2-IL1 and CH-IL1.

Fig. S2 Expression levels of *RsFTa* and *RsFTb* in G2-IL1 and CH-IL1.

Fig. S3 Relationship between days to bolting and *RsFTa* expression level in the F_2 population.

Fig. S4 Dot plot analysis of structural variations around *RsFLC1* (a) and *RsFLC3* (b) between the most similar reference genomes for G2-IL1 and CH-IL1.

Fig. S5 Integrated Genome Viewer (IGV) view of Oxford Nanopore long-read sequencing of CH-IL1 reads mapped to the RS08 genome.

Fig. S6 Number of opened flowers in cabbage scions grafted onto different genotypes of radish rootstocks.

Table S1. Distribution of $rsflc1^{Ldr1}$ and $rsflc3^{Rpn1}$ allele among diverse radish germplasms.

Table S2. Primers used in this study.

Table S3 Summarized data for F_2 population and their parents for linkage map construction and QTL analysis.

Table S4 Summary of the F_2 population linkage map.

Table S5. Differentially expressed genes identified between G2-IL1 and CH-IL1 by RNA-seq analysis.

Table S6. Summarized data for RNA-seq, short-read resequencing and Oxford Nanopore sequencing.

Data S1 Genotypic information of the F_2 population.

References

Ashworth MB, Walsh MJ, Flower KC, Vila-Aiub MM, Powles SB (2016) Directional selection for flowering time leads to adaptive evolution in *Raphanus raphanistrum* (wild radish). *Evolutionary Applications* 9: 619–629

Bolger AM, Lohse M, Usadel B (2014) Trimmomatic: a flexible trimmer for Illumina sequence data. *Bioinformatics* 30: 2114–2120

Broman KW, Wu H, Sen S, Churchill GA (2003) R/qtl: QTL mapping in experimental crosses. *Bioinformatics* 19: 889–890

Bull SE, Alder A, Barsan C, Kohler M, Hennig L, Gruissem W, et al. (2017) FLOWERING LOCUS T triggers early and fertile flowering in glasshouse cassava (*Manihot esculenta* Crantz). *Plants* 6: 22

Bouché F, Lobet G, Tocquin P, Périlleux C (2016) FLOR-ID: an interactive database of flowering-time gene networks in *Arabidopsis thaliana*. *Nucleic Acids Research* 44: D1167–D1171

Calderwood A, Lloyd A, Hepworth J, Tudor EH, Jones DM, Woodhouse S, Bilham L, et al. (2021) Total *FLC* transcript dynamics from divergent paralogue expression explains flowering diversity in *Brassica napus*. *New Phytologist* 229: 3534–3548

Castillejo C, Pelaz S (2008) The balance between CONSTANS and TEMPRANILLO activities determines *FT* expression to trigger flowering. Curr Biol 18: 1338–1343.

595 Charbonneau A, Tack D, Lale A, Goldston J, Caple M, Conner E, Barazani O, et al. (2018) Weed evolution: genetic
596 differentiation among wild, weedy, and crop radish. Evol Appl 11: 1964–1974
597 Chailakhyan MK (1936) New facts in support of the hormonal theory of plant development. *Comptes Rendus de*
598 *l'Académie des Sciences de l'URSS* 13: 79–83
599 Chen S (2023) Ultrafast one-pass FASTQ data preprocessing, quality control, and deduplication using fastp. *iMeta* 2:
600 e107. https://doi.org/10.1002/imt2.107
601 Choi K, Kim J, Hwang HJ, Kim S, Park C, Kim SY, Lee I (2011) The FRIGIDA complex activates transcription of *FLC*,
602 a strong flowering repressor in *Arabidopsis*, by recruiting chromatin modification factors. *Plant Cell* 23: 289–303
603 Cingolani P, Platts A, Wang LL, Coon M, Nguyen T, Wang L, Land SJ, Lu X, Ruden DM (2012) A program for
604 annotating and predicting the effects of single nucleotide polymorphisms, SnpEff: SNPs in the genome of
605 *Drosophila melanogaster* strain w1118; iso-2; iso-3. *Fly* 6: 80–92
606 Corbesier L, Vincent C, Jang S, Fornara F, Fan Q, Searle I, et al. (2007) FT protein movement contributes to long-
607 distance signaling in floral induction of *Arabidopsis*. *Science* 316: 1030–1033
608 Curtis GJ (1964) Graft transmission of the flowering stimulus from a wild *Beta* species to a line of beet selected for
609 resistance to bolting. *Nature* 203: 201–202
610 Curtis GJ, Hornsey KG (1964) Graft-transmissible induction of elongation and flowering in scions of sugar-beet bred for
611 resistance to bolting. *Nature* 202: 1238
612 Danecek P, Bonfield JK, Liddle J, Marshall J, Ohan V, Pollard MO, Whitwham A, et al. (2021) Twelve years of
613 SAMtools and BCFtools. *GigaScience* 10: giab008
614 Fujise K (1964) Studies on flowering, fruiting, and self- and cross-incompatibility in sweet potato varieties. *Bull Kyushu*
615 *Agric Exp Stn* 9: 123–246 (in Japanese)
616 Garner W, Allard H (1920) Effect of the relative length of day and night and other factors of the environment on growth
617 and reproduction in plants. *J Agric Res* 18: 553–606
618 Thorvaldsdóttir H, Robinson JT, Mesirov JP (2013) Integrative Genomics Viewer (IGV): high-performance genomics
619 data visualization and exploration. *Brief Bioinform* 14: 178–192
620 Helliwell CA, Wood CC, Robertson M, Peacock WJ, Dennis ES (2006) The Arabidopsis FLC protein interacts directly
621 in vivo with SOC1 and FT chromatin and is part of a high-molecular-weight protein complex. *Plant J* 46: 183–192
622 Hepworth J, Antoniou-Kourounioti RL, Berggren K, Selga C, Tudor EH, Yates B, Cox D, Harris BRC, Irwin JA,
623 Howard M, Säll T, Holm S, Dean C (2020) Natural variation in autumn expression is the major adaptive
624 determinant distinguishing Arabidopsis FLC haplotypes. *eLife* 9: e57671
625 Herzeel C, Costanza P, Decap D, Fostier J, Wuyts R, Verachtert W (2021) Multithreaded variant calling in elPrep 5.
626 *PLoS One* 16: e0244471
627 Huang C, Sun H, Xu D, Chen Q, Liang Y, Wang X, Xu G, et al. (2018) ZmCCT9 enhances maize adaptation to higher
628 latitudes. *Proc Natl Acad Sci USA* 115: E334–E341

629 Irwin JA, Soumpourou E, Lister C, Ligthart JD, Kennedy S, Dean C (2016) Nucleotide polymorphism affecting FLC
630 expression underpins heading date variation in horticultural brassicas. *Plant J* 87: 597–605
631 Jugulam M, Walsh M, Hall JC (2014) Introgression of phenoxy herbicide resistance from Raphanus raphanistrum into
632 Raphanus sativus. *Plant Breed* 133: 489–492
633 Kamitani M, Kashima M, Tezuka A, Nagano AJ (2019) Lasy-Seq: A high-throughput library preparation method for
634 RNA-Seq and its application in the analysis of plant responses to fluctuating temperatures. *Sci Rep* 9: 7091
635 Kashima M, Shida Y, Yamashiro T, Hirata H, Kurosaka H (2021) Intracellular and intercellular gene regulatory network
636 inference from time-course individual RNA-Seq. *Front Bioinform* 1: 777299
637 Kebaso L, Frimpong D, Iqbal N, Bajwa AA, Namubiru H, Ali HH, Ramiz Z, Hashim S, Manalil S, Chauhan BS (2020)
638 Biology, ecology and management of Raphanus raphanistrum L.: A noxious agricultural and environmental weed.
639 *Environ Sci Pollut Res Int* 27: 17692–17705
640 King RW, Hisamatsu T, Goldschmidt EE, Blundell C (2008) The nature of floral signals in *Arabidopsis*. I.
641 Photosynthesis and a far-red photoresponse independently regulate flowering by increasing expression of
642 *FLOWERING LOCUS T* (*FT*). *J Exp Bot* 59: 3811–3820
643 Kinoshita A, Richter R (2020) Genetic and molecular basis of floral induction in *Arabidopsis thaliana*. *J Exp Bot* 71:
644 2490–2504
645 Kinoshita Y, Motoki K, Hosokawa M (2023) Upregulation of tandem duplicated *BoFLC1* genes is associated with the
646 non-flowering trait in *Brassica oleracea* var. *capitata*. *Theor Appl Genet* 136: 41
647 Kitamoto N, Yui S, Nishikawa K, Takahata Y, Yokoi S (2014) A naturally occurring long insertion in the first intron in
648 the *Brassica rapa FLC2* gene causes delayed bolting. *Euphytica* 196: 213–223
649 Kobayashi M, Nakanishi T (1982) Flower induction by top-grafting in sweet potato. *Proc 5th Int Symp Trop Root Tuber*
650 *Crops*: 49–58
651 Lam SL, Cordner HB (1955) Flowering hormone in relation to blooming in sweetpotatoes. *Science* 121: 140–141.
652 Lang A (1952) Physiology of flowering. *Annu Rev Plant Physiol* 3: 265–306
653 Li H (2018) Minimap2: pairwise alignment for nucleotide sequences. *Bioinformatics* 34: 3094–3100
654 Li H, Durbin R (2009) Fast and accurate short read alignment with Burrows-Wheeler transform. *Bioinformatics* 25:
655 1754–1760
656 Li H, Handsaker B, Wysoker A, Fennell T, Ruan J, Homer N, Marth G, Abecasis G, Durbin R, 1000 Genome Project
657 Data Processing Subgroup (2009) The Sequence Alignment/Map format and SAMtools. *Bioinformatics* 25: 2078–
658 2079
659 Li X, Zhang S, Bai J, He Y (2016) Tuning growth cycles of *Brassica* crops via natural antisense transcripts of *BrFLC*.
660 *Plant Biotechnol J* 14: 905–914
661 Li LZ, Xu ZG, Chang TG, Wang L, Kang H, Zhai D, Zhang LY, et al. (2023) Common evolutionary trajectory of short
662 life-cycle in Brassicaceae ruderal weeds. Nat Commun 14: 290.

Lifschitz E, Eviatar T, Rozman A, Shalit A, Goldshmidt A, Amsellem Z, et al. (2006) The tomato *FT* ortholog triggers systemic signals that regulate growth and flowering and substitute for diverse environmental stimuli. *Proc Natl Acad Sci USA* 103: 6398–6403

Lin MK, Belanger H, Lee YJ, Varkonyi-Gasic E, Taoka KI, Miura E, et al. (2007) *FLOWERING LOCUS T* protein may act as the long-distance florigenic signal in the cucurbits. *Plant Cell* 19: 1488–1506

Liu L, Adrian J, Pankin A, Hu J, Dong X, von Korff M, Turck F (2014) Induced and natural variation of promoter length modulates the photoperiodic response of *FLOWERING LOCUS T*. *Nat Commun* 5: 4558

Marçais G, Delcher AL, Phillippy AM, Coston R, Salzberg SL, Zimin A (2018) MUMmer4: a fast and versatile genome alignment system. *PLoS Comput Biol* 14: e1005944

Michaels SD, Amasino RM (1999) *FLOWERING LOCUS C* encodes a novel MADS domain protein that acts as a repressor of flowering. *Plant Cell* 11: 949–956

Mitsui Y, Yokoyama H, Nakaegawa W, Tanaka K, Komatsu K, Koizuka N, Okuzaki A, Matsumoto T, Takahara M, Tabei Y (2023) Epistatic interactions among multiple copies of *FLC* genes with naturally occurring insertions correlate with flowering time variation in radish. *AoB Plants* 15: plac066

Mizuno N, Toyoshima M, Fujita M, Fukuda S, Kobayashi Y, Ueno M, Tanaka K, Tanaka T, Nishihara E, Mizukoshi H, Yasui Y, Fujita Y (2020) The genotype-dependent phenotypic landscape of quinoa in salt tolerance and key growth traits. *DNA Res* 27: dsaa022

Motoki K, Kinoshita Y, Hosokawa M (2019) Non-vernalization flowering and seed set of cabbage induced by grafting onto radish rootstocks. *Front Plant Sci* 9: 1967

Motoki K, Kinoshita Y, Nakano R, et al. (2022) Quantitative analysis of florigen for the variability of floral induction in cabbage/radish intergeneric grafting. *Plant Cell Physiol* 63: 1230–1241

Motoki K, Kinoshita Y, Nakano R, Hosokawa M, Nakazaki T (2024) Development of the “GRAFT method”, a rapid floral induction technique of cruciferous crops by grafting onto radish rootstocks. *Regulation of Plant Growth & Development* 59: 46–54 (in Japanese)

Nakanishi T, Hinata K (1975) Self-seed production by CO_2 gas treatment in self-incompatible cabbage. *Euphytica* 24: 117–120

Nishikawa M, Tamiru-Oli M, Hara M, et al. (2023) Non-vernalization requirement for flowering in *Brassica rapa* conferred by a dominant allele of *FLOWERING LOCUS T*. *Theor Appl Genet* 136: 132

Nishimura K, Kokaji H, Motoki K, Yamazaki A, Nagasaka K, Mori T, Takisawa R, et al. (2024) Degenerate oligonucleotide primer MIG-seq: an effective PCR-based method for high-throughput genotyping. *Plant J* https://doi.org/10.1111/tpj.16708

Notaguchi M, Abe M, Kimura T, Daimon Y, Kobayashi T, Yamaguchi A, et al. (2008) Long-distance, graft-transmissible action of Arabidopsis *FLOWERING LOCUS T* protein to promote flowering. *Plant Cell Physiol* 49: 1645–1658

Odipio J, Getu B, Chauhan RD, Alicai T, Bart R, Nusinow DA, et al. (2020) Transgenic overexpression of endogenous *FLOWERING LOCUS T*-like gene *MeFT1* produces early flowering in cassava. *PLoS One* 15: e0227199

Ogiso-Tanaka E, Matsubara K, Yamamoto S, Nonoue Y, Wu J, Fujisawa H, Ishikubo H, et al. (2013) Natural variation of the *RICE FLOWERING LOCUS T 1* contributes to flowering time divergence in rice. *PLoS One* 8: e75959

Okazaki K, Sakamoto K, Kikuchi R, Saito A, Togashi E, Kuginuki Y, Matsumoto S, Hirai M (2007) Mapping and characterization of *FLC* homologs and QTL analysis of flowering time in *Brassica oleracea*. *Theor Appl Genet* 114: 595–608

Patro R, Duggal G, Love MI, Irizarry RA, Kingsford C (2017) Salmon provides fast and bias-aware quantification of transcript expression. *Nat Methods* 14: 417–419

Putterill J, Varkonyi-Gasic E (2016) *FT* and florigen long-distance flowering control in plants. *Curr Opin Plant Biol* 33: 77–82

Rastas P (2017) Lep-MAP3: robust linkage mapping even for low-coverage whole genome sequencing data. *Bioinformatics* 33: 3726–3732

R Core Team (2023) R: a language and environment for statistical computing. R Foundation for Statistical Computing, Vienna, Austria. https://www.R-project.org/

Robinson MD, McCarthy DJ, Smyth GK (2010) edgeR: a Bioconductor package for differential expression analysis of digital gene expression data. *Bioinformatics* 26: 139–140

Sheldon CC, Conn AB, Dennis ES, Peacock WJ (2002) Different regulatory regions are required for the vernalization-induced repression of *FLOWERING LOCUS C* and for the epigenetic maintenance of repression. *Plant Cell* 14: 2527–2537

Shi J, Tian Z, Lai J, Huang X (2023) Plant pan-genomics and its applications. Mol Plant 16: 168–186

Soares JM, Weber KC, Qiu W, Stanton D, Mahmoud LM, Wu H, et al. (2020) The vascular targeted citrus *FLOWERING LOCUS T3* gene promotes non-inductive early flowering in transgenic Carrizo rootstocks and grafted juvenile scions. *Sci Rep* 10: 1–18

Somerville GJ, Ashworth M, Beckie H (2024) Adaptations in wild radish (*Raphanus raphanistrum*) flowering time, Part 1: individual-based modeling of a polygenic trait. *Weed Sci* 72: 137–142

Soppe WJJ, Viñegra de la Torre N, Albani MC (2021) The diverse roles of FLOWERING LOCUS C in annual and perennial Brassicaceae species. *Front Plant Sci* 12: 627258

Suge H (1984) Nature of floral stimulus in *Perilla* as studied by grafting. I. Method of evaluation and the movement of floral stimulus as affected by N6-benzylaminopurine. *Jpn J Crop Sci* 53: 423–429

Takahashi Y, Teshima KM, Yokoi S, Innan H, Shimamoto K (2009) Variations in *Hd1* proteins, *Hd3a* promoters, and *Ehd1* expression levels contribute to diversity of flowering time in cultivated rice. *Proc Natl Acad Sci USA* 106: 4555–4560

Tang M, Bai X, Wang J, Chen T, Meng X, Deng H, et al. (2022) Efficiency of graft-transmitted *JcFT* for floral induction in woody perennial species of the *Jatropha* genus depends on transport distance. *Tree Physiol* 42: 189–201

Tränkner C, Lehmann S, Hoenicka H, Hanke MV, Fladung M, Lenhardt D, et al. (2010) Over-expression of an *FT*-homologous gene of apple induces early flowering in annual and perennial plants. *Planta* 232: 1309–1324

Ujibe K, Nishimura K, Kashima M, Hirata H (2021) Direct-TRI: high-throughput RNA-extracting method for all stages of zebrafish development. *Bio Protoc* 11: e4136

Van der Auwera GA, O'Connor BD (2020) *Genomics in the Cloud: Using Docker, GATK, and WDL in Terra*. O'Reilly Media, Sebastopol, CA

van de Pol PA (1972) Floral induction, floral hormones and flowering. *Meded Landbouwhogesch Wageningen* 72: 1–89

Wahl V, Ponnu J, Schlereth A, Arrivault S, Langenecker T, Franke A, Feil R, Lunn JE, Stitt M, Schmid M (2013) Regulation of flowering by trehalose-6-phosphate signaling in *Arabidopsis thaliana*. *Science* 339: 704–707

Wang Q, Zhang Y, Zhang L (2018) A naturally occurring insertion in the *RsFLC2* gene associated with late-bolting trait in radish (*Raphanus sativus* L.). *Mol Breed* 38: 11

Wang S, Li H, Li Y, Li Z, Qi J, Lin T, Yang X, Zhang Z, Huang S (2020) *FLOWERING LOCUS T* improves cucumber adaptation to higher latitudes. *Plant Physiol* 182: 908–918

Wenzel S, Flachowsky H, Hanke MV (2013) The fast-track breeding approach can be improved by heat-induced expression of the *FLOWERING LOCUS T* genes from poplar (*Populus trichocarpa*) in apple (*Malus* × *domestica* Borkh.). *Plant Cell Tissue Organ Cult* 115: 127–137

Wu Y, Ma Y, Wang M, Zhou H, Gan Z, Zeng R, et al. (2022) Mobility of *FLOWERING LOCUS T* protein as a systemic signal in trifoliate orange and its low accumulation in grafted juvenile scions. *Hortic Res* uhac056

Xia Z, Watanabe S, Yamada T, Tsubokura Y, Nakashima H, Zhai H, Anai T, et al. (2012) Positional cloning and characterization reveal the molecular basis for soybean maturity locus *E1* that regulates photoperiodic flowering. *Proc Natl Acad Sci USA* 109: E2155–E2164

Xu G, Tao Z, He Y (2022) Embryonic reactivation of FLOWERING LOCUS C by ABSCISIC ACID-INSENSITIVE 3 establishes the vernalization requirement in each *Arabidopsis* generation. *Plant Cell* 34: 2205–2221

Ye J, Geng Y, Zhang B, Mao H, Qu J, Chua NH (2014) The *Jatropha FT* ortholog is a systemic signal regulating growth and flowering time. *Biotechnol Biofuels* 7: 130

Yi G, Park H, Kim JS, Chae WB, Park S, Huh JH (2014) Identification of three *FLOWERING LOCUS C* genes responsible for vernalization response in radish (*Raphanus sativus* L.). *Hortic Environ Biotechnol* 55: 548–556 https://doi.org/10.1007/s13580-014-1151-x

Zeevaart JAD (1958) Flower formation as studied by grafting. *Meded Landbouwhogesch Wageningen* 58: 1–88

Zeevaart JAD (1976) Physiology of flower formation. *Annu Rev Plant Physiol* 27: 321–348

Zhang H, Harry DE, Ma C, Yuceer C, Hsu CY, Vikram V, et al. (2010) Precocious flowering in trees: the *FLOWERING LOCUS T* gene as a research and breeding tool in *Populus*. *J Exp Bot* 61: 2549–2560

Zhang X, Liu T, Wang J, Wang P, Qiu Y, Zhao W, Pang S, et al. (2021) Pan-genome of *Raphanus* highlights genetic variation and introgression among domesticated, wild, and weedy radishes. *Mol Plant* 14: 2032–2055

Zhao JJ, Kulkarni V, Liu NN, Del Carpio DP, Bucher J, Bonnema G (2010) *BrFLC2* (*FLOWERING LOCUS C*) as a candidate gene for a vernalization response QTL in *Brassica rapa*. *J Exp Bot* 61: 1817–1825

Zhao C, Takeshima R, Zhu J, Xu M, Sato M, Watanabe S, Kanazawa A, et al. (2016) A recessive allele for delayed flowering at the soybean maturity locus *E9* is a leaky allele of *FT2a*, a *FLOWERING LOCUS T* ortholog. *BMC Plant Biol* 16: 20

Figure legends

Fig. 1. Phenotype data of F_2 population and their parents showing different grafting floral induction abilities. (a) Representative pictures of cabbage scions grafted onto CH-IL1 and G2-IL1 radish rootstocks. The pictures were taken at 63 days after grafting. The cabbage grafted onto CH-IL1 started flowering while the cabbage grafted onto G2-IL1 continued vegetative growth. White arrowheads indicate graft junction. Scale bars = 10 cm. (b) A histogram of days to bolting in the radish F_1 and F_2 population and its parental accessions. (c) A histogram of the expression level of *RsFTa* in the leaf of the radish F_1 and F_2 population and its parental accessions at two weeks after sowing.

Fig. 2. The QTL analysis of the F_2 population. (a) LOD scores of QTLs for the days to bolting. (b) LOD scores of QTLs for the expression level of *RsFTa*. The red lines in (a), (b) and (c) indicate LOD score thresholds. (c) Enlarged pictures for *qFTexp3* and *qFTexp7*. The vertical lines on the x-axis show the position of markers. The gray bar shows a 1.5-LOD support interval. (d) An effect plot for the expression level of *RsFTa* in the F_2 population categorized by markers close to the LOD score peaks for *qFTexp3* and *qFTexp7*, with G2/G2, CH/CH, and G2/CH indicating the homozygous G2-IL1 allele, homozygous CH-IL1 allele, and heterozygous allele, respectively. Error bars indicate mean ± SE.

Fig. 3. Identification of the candidate genes for *qFTexp3* and *qFTexp7* by RNA-seq analysis and whole genome re-sequence analysis. (a) Integration of QTL analysis, RNA-seq analysis and whole genome re-sequence analysis for *qFTexp3* and *qFTexp7*. ***** Number of genes with polymorphisms between G2-IL1 and CH-IL1 which were annotated as HIGH or MODERATE for impact in SnpEff analysis of whole genome resequencing data. (b) List of differentially expressed genes (DEGs) between G2-IL1 and CH-IL1 that are predicted to be homologs of upstream regulator genes of *FT* in Arabidopsis (FDR = 0.05). The blue heatmap in the upper panel and the red heatmap in the lower panel indicate the homologs of genes with negative and positive effects on expression of *FT* in Arabidopsis, respectively. [z]Transcript id is the name of the transcript in the RS00 reference genome. [y]Chr shows chromosome. [x]Pos indicates the transcription start site for each gene in the RS00 reference genome. [w]Gene name indicates the Arabidopsis gene with the highest homology. (c) Expression level of the three *FLC* homologs in the RNA-seq data. The results of the Wilcoxon test between G2-IL1 and CH-IL1 are shown in the graph (n=4).

Fig. 4. Characterization of genomic sequences of *RsFLC1* and *RsFLC3*. (a, b) Number of homozygous polymorphisms against 11 radish reference genomes within the open reading frame (ORF) of *RsFLC1* (a) and *RsFLC3* (b) in the whole genome resequencing data. Orange shading indicates the lowest number of polymorphisms in each accession. (c, d) Analysis of structural variations around *RsFLC1* (c) and *RsFLC3* (d) between the most similar reference genomes for G2-IL1 and CH-IL1. The syntenic relationships between the two genomes are visualized based on the dot plot analysis. For simplicity, small structural variations are omitted in (c). The gene models in the corresponding regions are visualized based on the GFF files of each reference genome using Integrative Genomics Viewer. (e, f) Polymorphisms in the promoter regions of *RsFLC1* (e) and *RsFLC3* (f) between G2-IL1 and CH-IL1 alleles. (g) Electrophoresis images of the amplified products by multi-plex PCR using the primer sets shown in Fig. S1 for *RsFLC1* and *RsFLC3*, respectively. White and black arrowheads indicate the amplicon size expected from G2-IL1 and CH-IL1 allele, respectively. (h) An effect plot for the days to bolting in the F_3 population categorized by the above mentioned primer sets for *RsFLC1* and *RsFLC3*, with G2/G2, CH/CH, and G2/CH indicating the homozygous G2-IL1 allele, homozygous CH-IL1 allele, and heterozygous allele, respectively. Error bars indicate mean ± SE.

Fig. 5. Effect of *RsFLC1* and *RsFLC3* alleles on the floral induction ability of radish rootstocks. (a) Days to bolting after sowing of the radish rootstocks themselves. (b) Total area of leaves left on rootstocks after grafting at the day of grafting. (c–e) Time-course gene expression of (c) *RsFTa*, (d) *RsFLC1*, and (e) *RsFLC3* in the leaves of radish rootstocks used for the grafting experiment. At each time point, leaf disks were sampled from the largest non-yellowing leaves of each rootstock plant. *RsActin* was used as an internal control. Error bars indicate mean ± SE (n = 4–5). Arrowheads in the *RsFTa* graph indicate the average time point of grafting for each rootstock genotype. (f) Representative pictures of cabbage scions grafted onto F_2 individuals with different combination of *RsFLC1* and *RsFLC3* alleles. The pictures were taken at 65 days after grafting. White arrowheads indicate graft junction. Scale bars = 10 cm. (g) Floral status of the grafted scions at 65 days after grafting. (h) Days to flowering after grafting of the cabbage grafted onto F_2 individuals. ED: end of experiment; NF: non-flowering. Different letters indicate statistical difference among the treatments with pairwise Wilcoxon tests with the Bonferroni adjustment for multiple comparisons ($P < 0.05$, n = 7–10) in (a), (b) and (h).

Fig. 6. Distribution of *FLC* loss-of-expression alleles in radish germplasm. (a) Summary of the genotyping of diverse *R. sativus* and *R. raphanistrum* accessions. (b) Heterozygous state of *FLC* loss-of-expression alleles in the original cultivar used to develop CH-IL1. Black arrowheads indicate the bands corresponding to $rsflc1^{Ldrl}$ and $rsflc3^{Rpnl}$ alleles, and white arrowheads indicate the bands corresponding to $RsFLC1^{Lpt1}$ and $RsFLC3^{Ngr1}$. The smaller bands in the *RsFLC3* result, indicated by gray arrowheads, represent amplicons derived from an allele type other than $rsflc3^{Rpnl}$ or $RsFLC3^{Ngr1}$. Asterisks indicate individuals carrying heterozygous loss-of-expression *FLC* alleles.

Fig. 7. A proposed model for successful graft-mediated floral induction using radish rootstocks. (a) At high levels of *FLC* expression, *FT* expression is strongly repressed, and neither the radish rootstock nor the grafted cabbage scion undergoes

flowering. (b) A moderate reduction in *FLC* expression initiates *FT* expression, enabling flowering of the rootstock itself; however, this *FT* level remains insufficient to stably induce flowering in the grafted cabbage scion. (c) A further reduction in *FLC* expression results in a substantial increase in *FT* expression, which exceeds the threshold required to reliably induce flowering in the scion. This model implies that natural variation in other upstream regulators of *FT* may also influence the stability of graft-mediated floral induction.

Supplementary Files

This is a list of supplementary files associated with this preprint. Click to download.

- Sup.DataMotokietal..xlsx
- Sup.FigsMotokietal..pdf
- Sup.TablesMotokietal..xlsx